Reevaluation of thermal maturity and stages of petroleum formation of the Mississippian Barnett Shale, Fort Worth Basin, Texas

M. D. Lewan and M. J. Pawlewicz

ABSTRACT

New data including measured reflectance (%R_o), programmed open-system pyrolysis data, and kerogen elemental analyses obtained on the Mississippian Barnett Shale in the Fort Worth Basin, Texas, indicate that secondary-gas generation starts at 1.5% R_o and not at the previously prescribed 1.1% R_o. Oil-cracking kinetic parameters derived from pyrolysis experiments in the presence and absence of water indicate that secondary-gas generation will not occur at a thermal maturity as low as 1.1% R_o and requires a minimum thermal maturity of 1.5% R_o. This difference is especially important in using the Barnett Shale as an analog for evaluating other possible shale-gas plays. The new reflectance measurements have a good relationship with hydrogen indices (HIs) and compare well with other published data sets. However, the relationship does not compare well with the previously published data used to prescribe 1.1% R_o as the start of secondary-gas generation in the Barnett Shale. This discrepancy is attributed to differences in measured %R_o values and not attributed to differences in the HI values. Lack of publicly available information on the previously reported %R_o values makes it difficult to ascertain the reason for their lower values. These lower %R_o values also have impact on the previously prescribed relationship for estimating %R_o from the temperature at maximum yield by programmed open-system pyrolysis (T_{max}). As a result, the new data do not agree with a previously described relationship, and the considerable scatter makes the new relationship unreliable. However, the relationship between the HI and %R_o has less scatter, which indicates that HI offers a better proxy in calculating %R_o than T_{max} for the Barnett Shale. Comparison of

Manuscript received March 25, 2016; provisional acceptance May 16, 2016; revised manuscript received November 2, 2016; final acceptance January 25, 2017.
DOI:10.1306/01251716053

AUTHORS

M. D. Lewan ~ *US Geological Survey (Emeritus), Denver Federal Center, P.O. Box 25046 MS 977, Denver, Colorado 80225; mlewan@usgs.gov and mlewan1@comcast.net*

Mike Lewan is a geochemist and geologist with more than 45 years of experience, including employment with Shell Oil Company in their New Orleans offshore exploration and production group, Amoco Production Company at their Tulsa Research Center, and US Geological Survey in their Central Energy Resources Team. He received his Ph.D. from the University of Cincinnati, his M.S. from Michigan Technological University, and his B.S. from Northern Illinois University.

M. J. Pawlewicz ~ *US Geological Survey (Retired), Denver Federal Center, P.O. Box 25046 MS 977, Denver, Colorado 80225; mark_pz@hotmail.com*

Mark Pawlewicz has been an organic petrologist and geologist for the US Geological Survey since 1979 and is involved in geochemistry, geology, and thermal-maturity studies of domestic and international source rocks related to resource assessments and applied research. He received a B.A. degree in geology from Pennsylvania State University and an M.S. from the Colorado School of Mines.

ACKNOWLEDGMENTS

The input of samples by petroleum companies was invaluable to this study, and the authors are particularly grateful to Todd Stephenson, John Sharp, and Don Harville at Chesapeake Energy; Bob Olson and Jeremy Rollins at Devon Energy; David Trice, John Chapman, Dan Jarvie, and Robert Garrison at EOG Resources; and John Callanan at Quicksilver Energy. The authors appreciate Dan Jarvie providing the data previously used to map vitrinite reflectance and the accompanying Rock-Eval data. Augusta Warden at the US Geological Survey (USGS) did an outstanding job of coordinating the outsourcing of analyses and conducting elemental analysis of isolated kerogen. Mark Dreier's determination of $\delta^{13}C$ of kerogen is also appreciated. Map construction and displays are the conscientious work of USGS

contractors Chris Anderson, Elena Stieve, and Wayne Husband.

The authors are appreciative of USGS editorial comments by Janet Slate and USGS technical review by Paul Hackley; AAPG technical and editorial reviews by Irene Arango, Barry Katz, and Michael Sweet were especially appreciated and helpful in improving the clarity and scientific content of the original manuscript. Any use of trade, firm, or product names is for descriptive purposes only and does not imply endorsement by the US government.

various programmed open-system pyrolysis methods (i.e., Rock-Eval II, Rock-Eval 6, Source Rock Analyzer, and Hawk) indicates that variations in HI are within ±10% of one another. An HI of at least 44 mg/g total organic carbon is prescribed as a more certain limit for the start of secondary-gas generation and prospective in situ gas-shale accumulations.

INTRODUCTION

The Mississippian Barnett Shale in the Fort Worth Basin of Texas represents the type shale-gas play (Pollastro, 2007). Although this unconventional gas play may commonly be used as an analog for exploration on a global scale (Jarvie, 2012), it is not completely understood as a petroleum system. A regional map of vitrinite reflectance (%R_o) of the Barnett Shale has been published (Pollastro et al., 2007). However, its utility depends on whether "suppressed vitrinite" or solid bitumen common in Paleozoic source rocks is being measured (Price and Barker, 1985; Buchardt and Lewan, 1990) and how the reflectance values (%R_o) relate to various stages of petroleum formation (Lewan, 1985). Vitrinite reflectance is a critical parameter in determining the amount of thermal stress (temperature and time) a source rock experienced during its burial, but this does not always correlate consistently with stages of petroleum formation.

Stages of petroleum formation for an oil-prone source rock like the Barnett Shale include oil, primary-gas, and secondary-gas generation. Start of oil generation occurs with the thermal decomposition of high-molecular-weight polar-rich bitumen derived from the partial decomposition of the original kerogen in a source rock (Maier and Zimmerly, 1924; Tissot, 1969; Lewan et al., 1985). Hydrocarbon-rich oil generated during this stage is immiscible in the dissolved-water–bearing bitumen (Lewan, 1997). This hydrocarbon-rich oil is either expelled to source conventional-oil accumulations or retained to source unconventional-oil accumulations. Any combination of these two end members may occur depending on the amount and type of organic matter, level of thermal maturity, and rock properties of a maturing source rock. The start and end of oil generation may occur over a wide range of thermal-stress levels as measured by R_o. This variability in thermal stress depends on kerogen type and organic-sulfur content (Lewan, 1985; Tissot et al., 1987). Start of oil generation from high-sulfur type IIS kerogen has been reported to be as low as 0.3% R_o (Petersen and Hickey, 1987), and end of oil generation for low-sulfur type II kerogen can occur as high as 1.3% R_o based on laboratory kinetics (Lewan and Ruble, 2002). This upper limit for oil generation from type II kerogen is also in general agreement with that proposed by Vassorvich et al. (1974) and Dow and O'Conner (1982). Primary-gas generation starts concurrently

with oil generation as kerogen converts to bitumen and bitumen converts to oil. Precursory sources of primary gas within the decomposing kerogen and bitumen are sufficient for this stage to extend beyond the end of oil generation but are limited to thermal stress levels less than 2.0% R_o (Lewan and Kotarba, 2014). Hydrocarbon-rich oil retained in a source rock or expelled into traps that remain coherent with burial depth will thermally decompose into secondary gas and pyrobitumen at elevated thermal stress levels. Kinetic models based on laboratory pyrolysis indicate that secondary-gas generated from oil cracking starts at a minimum of 1.5%–1.7% R_o (Schenk et al., 1997; Tsuzuki et al., 1999). These same kinetic models indicate that the end of secondary-gas generation occurs between 3.3% and 3.9% R_o depending on whether the oil is in a water-wet or oil-wet reservoir, respectively.

Within the thermal stress levels of these stages of petroleum formation, it is difficult to rationalize the interpretation that secondary-gas generation in the Barnett Shale commences at a 1.1% R_o as prescribed by Hill et al. (2007), Jarvie et al. (2007, their figure 11), and Pollastro (2007). With the exception of some high-sulfur type IIS kerogens, this value of 1.1% R_o is still within the range of oil generation, which can extend to a value of 1.3% R_o according to Dow and O'Conner (1982).

The objective of this study is to reevaluate stages of petroleum formation within the Barnett Shale using measured reflectance values on additional well samples in conjunction with geochemical parameters more indicative of petroleum formation (e.g., kerogen atomic H/C ratios and programmed open-system pyrolysis hydrogen indices [HIs]). Through a collaborative effort with Chesapeake Energy, EOG Resources, Devon Energy, Quicksilver Resources, and the US Geological Survey (USGS), 104 samples of the Barnett Shale were collected from 92 wells and 1 outcrop within the Fort Worth Basin (Table 1). These new data on these samples were supplemented with available HI data on samples from 56 wells reported by Pollastro et al. (2007) and 42 wells reported by Klentzman (2009). As shown by the sample locations and sources in Figure 1, the collaborative effort allowed for construction of a more complete thermal-maturity map, which would not be possible with any of the individual data sets.

DATA SETS AND METHODS

US Geological Survey Data Set

The USGS data set consists of 94 samples of the Barnett Shale that were collected from 92 wells operated by Chesapeake Energy, EOG Resources, Devon Energy, or Quicksilver Resources and two samples from one outcrop within the Fort Worth Basin (Table 1). The two outcrop samples are from a quarry in Chapel Hill south of San Saba, Texas, on the east side of Farm to Market Road 1031. These samples are from the quarry floor and considered unweathered based on the presence of pyrite and the absence of saprolite rinds (Lewan, 1980); 7 of the well samples are from cores, 79 samples are from horizontal-well cuttings, and 6 samples are from vertical-well cuttings. Cuttings were composited until 100 to 200 g of sample were collected. During collection the cuttings were examined for contaminants, which included plastic spherical lubricant beads (Rayborn, 1977) and wood fragments. These contaminants were removed by a density separation using a 20 wt. % NaCl solution, which has a density of 1.15 g/cm^3. Plastic spherical lubricant beads and wood debris typically have densities less than 1.15 g/cm^3 (e.g., 1.03 to 1.06 and 0.35 to 0.75 g/cm^3, respectively). The procedure involved placing approximately 100 g of the cuttings with 400 ml of 20 wt. % NaCl solution in 800-ml polypropylene centrifuge bottles. The contents are mixed with a plastic stirring rod and then centrifuged for 10 min at 1500 rpm. The solution is decanted with any floating wood debris, plastic spherical lubricant beads, fine dust, or diesel oil. This procedure is repeated four additional times with tap water to remove residual NaCl solution on the samples. The rinsed cuttings are then transferred with distilled water to a two-piece Büchner polypropylene funnel with a Whatman GF/D glass microfiber filter (70-mm diameter). While filtering, an additional 100 ml of distilled water are passed over the cuttings as a final rinse. The cup piece with the rinsed cuttings is detached from the bottom funnel piece and placed in a vacuum oven at 70°C for 16 to 20 hr. The dried cuttings are pulverized in a puck and ring shatter box.

Total organic carbon (TOC) was determined with a Leco carbon analyzer, and HI was determined using the Leco TOC and generated petroleum (S_2) from Rock-Eval II pyrolysis (i.e., S_2/TOC × 100).

Table 1. Location, Leco Total Organic Carbon, and Rock-Eval II Analyses and Type of Barnett Samples in the US Geological Survey Data Set (All cuttings went through 20 wt. % NaCl treatment before analyses.)

Sample Number	Well API Number	Well Name and Number	TOC (wt. %)	Rock-Eval II Analysis*							Rock Type†
				S_1	S_2	S_3	T_{max}	HI	OI	PI	
011	42251327120000	Panchasarp "A": 2H	3.13	1.03	0.81	0.40	425	26	13	0.56	CutH
012	42251337450000	Fielderdale: 1H	2.80	1.34	0.34	0.29	334	12	10	0.80	CutH
013	42251319020000	Little Hoss: T1H	3.22	1.45	1.09	0.31	447	34	10	0.57	CutH
014	42251313500000	Damsel Fly Nymph: 4H	4.03	2.71	1.04	0.20	452	26	5	0.72	CutH
015	42251317280000	Isbell: 2H	5.74	1.09	0.76	0.19	423	13	3	0.59	CutH
016	42113301330000	DFW: C4HH	4.16	0.88	0.58	0.15	393	14	4	0.60	CutH
017	42113301190000	Campbell: 1H	3.15	0.58	1.11	0.30	394	35	10	0.34	CutH
018	42113301070100	Danciger Trust: 1H	2.05	0.70	0.39	0.20	341	19	10	0.64	CutH
019	42439337610000	DFW: A5HE	4.42	1.31	0.40	0.23	335	9	5	0.77	CutH
020	42113301160000	DFW North: A5HN	4.45	1.54	0.29	0.30	323	7	7	0.84	CutH
021	42439325960000	Armet Dale Street South: 1H	4.03	2.86	0.67	0.15	335	17	4	0.81	CutH
022	42439325240000	Baptist Southwest: 1H	2.76	0.75	0.61	0.33	433	22	12	0.55	CutH
023	42439336650000	McCulley: 1H	3.78	0.89	0.55	0.28	434	15	7	0.62	CutH
024	42439335080000	Bright Star 1: 1H	3.68	2.99	0.94	0.19	434	26	5	0.76	CutH
025	42439338280000	AC Stone: 1H	3.62	3.63	1.09	0.17	365	30	5	0.77	CutH
026	42439321140000	Brentwood SWD: 1H	1.79	0.55	0.41	0.12	354	23	7	0.57	CutH
027	42439323750000	MEDC: 1H	3.59	1.15	0.39	0.28	328	11	8	0.75	CutH
028	42439334380000	TCCD south: 2H	4.42	1.59	0.64	0.25	442	14	6	0.71	CutH
029	42439346010000	Bruder: 1H	4.02	2.85	0.97	0.15	395	24	4	0.75	CutH
030	42439338320000	Grapevine Mills: 1H	4.47	2.53	0.62	0.22	332	14	5	0.80	CutH
031	42439346910000	Little Bear South: 1H	3.98	3.58	0.68	0.10	332	17	3	0.84	CutH
032	42121340310000	Dunn Clara Lyles: 15H	4.91	1.95	2.85	0.33	460	58	7	0.41	CutH
033	42121339660000	Biltmore: 10H	4.20	1.33	2.13	0.35	393	51	8	0.38	CutH
034	42121339390000	DCCO 3 Burns Anna Beth: 29H	5.27	1.09	3.83	0.13	407	73	2	0.22	CutH
035	42121338400000	Bradford John: 2H	3.91	0.93	1.96	0.49	462	50	13	0.32	CutH
036	42121340640000	DCCO 4-WCCO 1-DCCO 4 SA: 1H	3.99	0.42	0.62	0.26	463	16	7	0.40	CutH
037	42121324870000	Erickson Lena: 1H	1.91	0.19	0.72	0.42	453	38	22	0.21	CutH
038	42121326560000	Roanoke Ranch: 1H	4.14	1.38	0.75	0.29	336	18	7	0.65	CutH
039	42121326420000	Dunn Hobby D: 2H	1.25	0.06	0.24	0.24	463	19	19	0.20	CutH
040	42121330900000	Bohn Tina: 1H	4.28	1.37	3.87	0.61	448	90	14	0.26	CutH
041	42497347730000	Waggoner Merle T: 2	3.71	1.62	3.97	0.43	449	107	12	0.29	CutV
042	42497375240000	Barnes Joshua: 2H	4.34	3.64	9.83	0.81	444	226	19	0.27	CutH
043	42497369780000	Simpson W M: 5H	3.40	1.65	3.34	0.44	453	98	13	0.33	CutH
044	42497371480000	Robinson Elmer: 1H	3.42	0.99	3.98	0.67	443	116	20	0.20	CutH
045	42497372590000	Parsons F P Federal: 1H	4.00	2.25	6.56	0.69	441	164	17	0.26	CutH
046	42497370370000	Winkler O R gas unit: 1H	4.29	1.29	2.69	0.59	453	63	14	0.32	CutH
047	42497370430000	Fox Jeff-Fox Zina SA: 3H	1.00	0.26	0.40	0.56	436	40	56	0.39	CutH
048	42497365210000	Smith Ernest "A": 1H	4.10	1.26	3.96	0.67	449	97	16	0.24	CutH
049	42497356950000	Taylor R B: 6H	3.08	0.66	1.11	0.34	457	36	11	0.37	CutH
050	42497371150000	DCCO2-SHOOP "G"-DCCO2SA: 1H	5.20	0.77	2.58	0.48	463	50	9	0.23	CutH
051	42217303920000	Island Grove Ranch unit: 1H	3.66	0.74	0.95	0.35	402	26	10	0.44	CutH
052	42217303940000	Ellison unit: 1H	2.18	0.43	0.29	0.19	ND	13	9	0.60	CutH

(*continued*)

Table 1. Continued

Sample Number	Well API Number	Well Name and Number	TOC (wt. %)	Rock-Eval II Analysis*							Rock Type†
				S_1	S_2	S_3	T_{max}	HI	OI	PI	
053	42121326010000	Burch Marvin: 2H	2.77	0.65	0.41	0.30	543	15	11	0.61	CutH
054	42121324890000	Gunnels: 1H	3.55	0.55	0.33	0.37	544	9	10	0.63	CutH
055	42367337620000	Betts Edith Gas Unit: 1H	3.37	0.68	0.50	0.31	457	15	9	0.58	CutH
056	42497362120000	Dearing Marvin: 1H	3.54	0.61	0.99	0.41	456	28	12	0.38	CutH
057	42439311120000	Seybold Rethia: 2H	4.12	1.15	0.36	0.35	541	9	8	0.76	CutH
058	42497358550000	Kindle W A "A": 1H	5.04	1.44	0.59	0.42	546	12	8	0.71	CutH
059	42497361080000	Wison M S: 2H	1.13	0.30	0.52	0.31	450	46	27	0.37	CutH
060	42439315020000	Lester Lucille Gas unit: 1H	1.31	0.24	0.22	0.16	ND	17	12	0.52	CutH
061	42367343470000	Sugar Tree: 2H	3.49	1.37	2.56	0.61	448	73	18	0.35	CutH
062	42367339870000	Mona R Fields: 1H	3.26	0.93	1.07	0.38	449	33	12	0.47	CutH
063	42425301890000	Wasilchak: 2H	3.55	0.68	1.13	0.56	457	32	16	0.38	CutH
064	42367345760000	Frank Mask gas unit: 1H	2.70	0.96	1.68	0.46	454	62	17	0.36	CutH
065	42367340940000	Sugar Tree: 1H	3.79	1.54	3.08	0.46	457	81	12	0.33	CutH
066	42097341890000	A-1: 3H	1.53	2.72	1.96	0.80	423	128	52	0.58	CutH
067	42139304760000	Kutner unit: 2H	2.63	1.68	0.52	0.46	405	20	17	0.76	CutH
068	42237390300000	Wolfe Martha unit: 1H	4.33	1.59	7.92	0.60	444	183	14	0.17	CutH
069	42337348070000	Dobbs unit: 2H	5.86	17.41	11.53	0.75	444	197	13	0.60	CutH
070	42097340810000	Christian C unit: 7H	5.55	26.20	8.43	0.86	442	152	15	0.76	CutH
071	42363359320000	McMurrey: 1	3.92	4.92	2.88	0.69	456	73	18	0.63	CutV
072	42425301550000	Fain: 1H	4.00	4.03	3.69	0.63	445	92	16	0.52	CutH
073	42077349960000	Scaling Ranch G: 1	3.11	3.89	6.50	1.16	441	209	37	0.37	CutV
074	42337343040000	Alamo B unit: 6H	5.06	7.71	8.66	1.08	440	171	21	0.47	CutH
075	42337344920000	Pacific B unit: 1H	4.98	6.51	5.44	1.49	438	109	30	0.54	CutH
076	42363360230000	Lyons unit: 2	1.47	1.49	0.72	0.57	438	49	39	0.67	CutH
077	42217304410000	Tam: 1	1.88	1.77	1.06	0.64	425	56	34	0.63	CutV
078	42337345200000	Redman North: 2	4.08	4.63	7.38	1.27	436	181	31	0.39	CutH
079	42139304980000	Westside: 1H	4.11	5.34	2.78	0.93	425	68	23	0.66	CutH
080	42143310760000	Houston Ranch: 2H	3.31	2.61	3.42	0.61	444	103	18	0.43	CutH
081	42221310940000	Rhoades: 1H	3.30	1.19	1.16	0.62	450	35	19	0.51	CutH
082	42217304570000	Gordon SWD: 1	4.00	0.16	0.11	0.09	ND	3	2	0.59	CutV
083	42363357090000	Crawford: 3	4.19	3.22	3.54	0.35	456	84	8	0.48	CutH
084	42143312210000	Betty Thompson: 1H	1.37	0.77	0.78	0.23	447	57	17	0.50	CutH
085	42429364600000	Link Ranch: 1	3.00	1.93	1.68	0.81	444	56	27	0.53	CutV
086	42363359210000	Robertson Hill Ranch "B": 5	3.02	2.98	3.31	0.54	450	110	18	0.47	Core‡
087	42337339410000	Swint Paul: 1	4.85	4.12	12.94	0.51	447	267	11	0.24	Core‡
088	42251301450000	Two O Five: 2H	6.03	2.38	3.29	0.35	474	55	6	0.42	CutH
089	42251311110000	RAAM unit: 3	4.22	0.10	0.19	0.17	ND	5	4	0.34	Core‡
090	42221310010000	Black Ranch: 2	7.16	3.09	7.38	0.36	458	103	5	0.30	Core‡
091	42143311010000	French Ranch: 1	3.30	1.51	1.86	0.42	453	56	13	0.45	Core‡
092	42077350030000	Fuller: 1	5.26	1.83	13.14	0.33	450	250	6	0.12	Core‡
093	42077349710000	Scaling Ranch A: 1	6.60	5.19	17.19	0.52	448	260	8	0.23	Core‡

(*continued*)

Table 1. Continued

Sample Number	Well API Number	Well Name and Number	TOC (wt. %)	Rock-Eval II Analysis*							Rock Type†
				S_1	S_2	S_3	T_{max}	HI	OI	PI	
094	Chapel Hill Quarry	Field No. 080427-1	8.37	0.77	40.00	1.38	421	478	16	0.02	Otcp‡
095	Chapel Hill Quarry	Field No. 080427-2	7.92	0.44	37.19	1.11	421	470	14	0.01	Otcp‡
096	42221311840000	Boy Scout: 1H	1.33	0.86	1.07	0.34	429	80	26	0.45	CutH
097	42221310180000	Lucy unit: 1H	2.76	0.93	1.10	0.22	458	40	8	0.46	CutH
098	42035301220000	Marvel Girl: 1H	3.39	0.40	0.38	0.16	345	11	5	0.51	CutH
099	42425301590000	Drechsel unit: 2H	4.28	0.97	2.17	0.43	454	51	10	0.31	CutH
100	42035301250000	Nibbler unit: 1H	4.08	0.36	0.56	0.75	440	14	18	0.39	CutH
101	42217304290000	Sideshow Bob: 1H	2.57	0.30	0.27	0.25	533	11	10	0.53	CutH
102	42221318320000	Briscoe unit: 3H	3.89	1.90	3.57	0.25	454	92	6	0.35	CutH
103	42217305140000	Frances unit: 1H	4.35	3.49	2.58	0.55	410	59	13	0.57	CutH
104	42425302610000	Luminant: 2H	3.36	1.75	2.79	0.32	452	83	10	0.39	CutH

Abbreviation: TOC = total organic carbon.

*Rock-Eval parameters: HI = hydrogen index ($S_2 \times 100$/TOC); ND = not determined because of broad poorly resolved S_2 peak; OI = oxygen index ($S_3 \times 100$/TOC); PI = production index ($S_1/[S_1 + S_2]$); S_1 = volatile petroleum (mg/g rock); S_2 = generated petroleum (mg/g rock); S_3 = carbon dioxide generated (mg/g rock); T_{max} = temperature at maximum S_2 rate (°C).

†Rock type: CutH = cuttings from horizontal well; CutV= cuttings from vertical well; Otcp = outcrop.

‡AR = as received, no preparation; NaCl = density separation with 20 wt. % NaCl solution; Prep = preparation before analyses.

GeoMark Research conducted both of these analyses on aliquots of the pulverized samples. The significance of the 20 wt. % NaCl treatment of cuttings was evaluated by conducting Leco TOC and Rock-Eval II analyses on aliquots of 35 untreated samples (Table 2) for comparison. Figure 2 shows that in some cases the procedure was not necessary, with good agreement between the HI values, but in other cases the differences were significant. The largest differences are attributed to the presence of plastic spherical lubricant beads. To ensure consistency, the 20 wt. % NaCl treatment was used on all cutting samples irrespective of whether plastic spherical lubricant beads or wood debris were observed during sample collection.

Reflectance measurements were performed on a Zeiss reflected-light microscope, at 500× magnification with oil immersion. The microscope configuration meets all the criteria for organic-matter observation and reflectance measurement as stated in ASTM D7708 (ASTM, 2011). Sample preparation was minimized by using whole rock, with material from cuttings or core crushed by mortar and pestle to a size fraction between 0.1 and 2 mm. There was no treatment by any additional method(s). This rock material was mixed with low-viscosity epoxy and then allowed to set overnight. After curing, the pellets were ground with 60-grit and then 600-grit sandpaper, and then they were polished with a 0.3- and a 0.05-μm polish on a rotating lap, producing a scratch-free surface. Although reflectance of vitrinite macerals from the Barnett Shale has been reported (Pollastro et al., 2007; Klentzman, 2009), the distinction between reflectance of true vitrinite and suppressed vitrinite or solid bitumen is difficult (e.g., Buchardt and Lewan, 1990; Xiao et al., 2000). An interlaboratory reflectance-measurement study on dispersed organic matter found that reflectance values reported on bitumen by some petrographers were identical with those measured on vitrinite identified by other petrographers (Hackley et al., 2015). Measured reflectance values reported in Table 3 were made on individual organic entities dispersed in the rock matrix and elongate-shaped organic entities parallel to the bedding fabric. The measured organic entities visually resembled vitrinite in having a uniform reflectance, but in some cases their nonangular shape and pore-filling nature suggest solid bitumen. However, gelification of woody debris in vitrinite formation during early diagenesis (Chaffee et al., 1984; Russell, 1984; Hatcher et al., 1985; Stout and Spackman, 1987) suggests that these malleable protovitrinite gels can deform around mineral grains or fill pores when dispersed in sediments during early

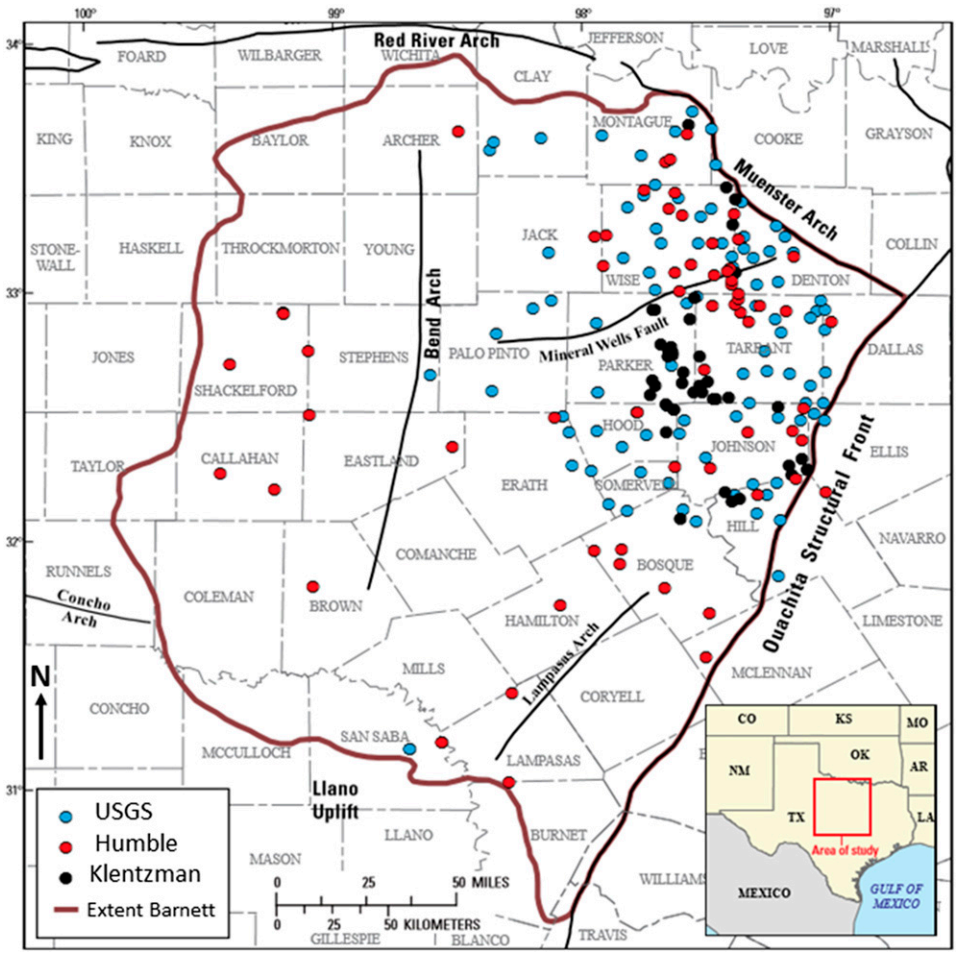

Figure 1. Map showing major structural features, extent of the Barnett Shale, and sample locations from three data sets in the Fort Worth Basin of Texas. AR = Arkansas; CO = Colorado; KS = Kansas; LA = Louisiana; MO = Missouri; NM = New Mexico; OK = Oklahoma; TX = Texas; USGS = US Geological Survey.

compaction. Some samples did reveal a rare occurrence of terrigenous organic matter in the form of inertinite and some recycled type II organic matter. No measurements were taken on these rare materials. The measured reflectance on these vitrinite-like macerals is deemed to be the same as that measured by earlier analysts and can be modeled with EASY% R_o (Sweeney and Burnham, 1990). As presented later, this claim is supported by comparable relationships between measured %R_o and HI values from reliable data previously published (i.e., Olson, 2008; Klentzman, 2009; Hackley et al., 2015). Each polished sample was scanned for organic matter, and one measurement was taken on any one entity with a minimum size of 5 μm. This highly selective procedure accounts for the low number of %R_o values made per sample but eliminates extraneous material deemed marginal with respect to size and physical character. It should be noted that measurements made by the coauthor (M. J. Pawlewicz) were within the margin of error for more than 80% of the analyses in the interlaboratory ASTM study of reflectance measurements on dispersed organic matter (Hackley et al., 2015). Lastly, all measurements were made independent of prior knowledge of Rock-Eval HI or temperature at maximum S_2 rate (T_{max}) values.

As noted by Baskin (1997) and Lewan et al. (2002), it is important to calibrate HI values determined on a source rock with the atomic H/C ratio of its isolated kerogen. This is important in determining the HI value above which no relationship with atomic H/C ratio occurs, which denotes preoil generation. Lewan et al. (2002) noted that oil generation from the Devonian–Mississippian New Albany Shale in the Illinois Basin occurred at HI values less than 450 mg S_2/g TOC. Calibration of atomic H/C ratios with HI in the Mississippian–Devonian Bakken Formation of the Williston Basin indicated that oil generation occurred at HI values less than 400 mg S_2/g TOC (Lewan, 2013). Variations in HI values greater than these values showed no relationship

Table 2. Leco Total Organic Carbon and Rock-Eval II Analyses of Selected Cutting Samples from the US Geological Survey Data Set That Were Not Treated with the 20 wt. % NaCl Solution

Sample Identification Number	TOC (wt. %)	Rock-Eval II Analysis*							Treated** Sample Number
		S_1	S_2	S_3	T_{max}	HI	OI	PI	
001	6.84	1.60	30.69	55.80	405	448.0	8.0	0.050	051
002	3.43	1.39	3.70	7.55	402	107.0	14.3	0.270	052
003	3.11	0.66	1.26	0.72	340	40.0	56.6	0.340	053
004	3.46	0.39	0.25	0.51	ND	7.0	14.2	0.610	054
005	2.91	0.64	0.52	1.58	492	17.0	11.3	0.550	055
006	3.40	0.94	1.34	2.39	453	39.4	16.5	0.410	056
007	4.13	1.68	0.62	1.19	429	15.0	12.6	0.730	057
008	4.83	1.45	2.15	2.99	451	44.5	14.9	0.400	058
009	1.38	0.38	1.16	1.63	455	84.1	51.5	0.250	059
010	3.05	0.37	0.61	1.39	493	20.0	14.4	0.380	060
105	2.80	0.94	0.52	0.44	473	18.6	15.7	0.644	013
106	4.31	2.81	1.13	0.33	485	26.2	7.7	0.713	014
107	3.66	0.81	1.58	0.47	401	43.2	12.8	0.339	017
108	3.86	2.32	0.57	0.22	501	14.8	5.7	0.803	021
109	3.71	0.46	0.39	0.26	479	10.5	7.0	0.541	023
110	3.99	2.66	0.77	0.27	439	19.3	6.8	0.776	024
111	2.26	2.59	0.52	0.29	343	23.0	12.8	0.833	025
112	3.21	0.71	0.15	0.30	ND	4.7	9.3	0.826	027
113	4.89	1.20	3.02	0.34	406	61.8	7.0	0.284	028
114	6.07	5.67	23.28	1.81	406	383.5	29.8	0.196	042
115	4.49	3.13	9.49	0.99	448	211.4	22.0	0.248	045
116	3.87	1.38	3.04	0.53	459	78.6	13.7	0.312	046
117	4.23	1.78	4.81	0.56	452	113.7	13.2	0.270	048
118	4.96	1.42	3.48	1.05	458	70.2	21.2	0.290	050
119	3.56	1.41	2.75	0.72	457	77.2	20.2	0.339	061
120	3.23	1.35	2.54	0.45	456	78.6	13.9	0.347	064
121	4.34	2.36	8.15	0.54	447	187.8	12.4	0.225	068
122	4.06	29.52	6.38	0.94	444	157.1	23.2	0.822	070
123	3.88	4.15	3.51	0.54	455	90.5	13.9	0.542	071
124	3.78	2.25	2.87	0.64	452	75.9	16.9	0.439	072
125	2.87	3.01	6.68	0.97	446	232.8	33.8	0.311	073
126	3.39	7.97	6.69	1.04	440	197.3	30.7	0.544	074
127	3.31	1.07	1.88	1.16	447	56.8	35.0	0.363	076
128	3.46	2.78	3.68	0.47	452	106.4	13.6	0.430	080
129	3.45	2.30	1.72	0.62	449	49.9	18.0	0.572	081
130	0.98	0.47	0.44	0.29	459	44.9	29.6	0.516	083
131	3.37	0.37	0.38	0.23	504	11.3	6.8	0.493	098
132	2.51	0.25	0.10	0.24	ND	4.0	9.6	0.714	101
133	3.60	1.82	3.58	0.28	455	99.4	7.8	0.337	102
134	4.08	2.54	3.48	0.46	457	85.3	11.3	0.422	104

Abbreviation: TOC = total organic carbon.

*Rock-Eval parameters: HI = hydrogen index ($S_2 \times 100$/TOC); ND = not determined because of broad poorly resolved S_2 peak; OI = oxygen index ($S_3 \times 100$/TOC); PI = production index ($S_1/[S_1 + S_2]$); S_1 = volatile petroleum (mg/g rock); S_2 = generated petroleum (mg/g rock); S_3 = carbon dioxide generated (mg/g rock); T_{max} = temperature at maximum S_2 rate (°C).

**Sample numbers from Table 1 of samples treated with 20 wt. % NaCl.

with changes in the composition of kerogen, which was also originally reported by Espitalié et al. (1977). In accordance with these studies, kerogen was isolated from a 16-sample subset that included the full range of HI values from 3 to 478 mg S_2/g TOC. The isolation procedure was that given by Lewan (1986), which involves dilute (6N) HCl; 49% HF; hot, concentrated (~12 N) HCl; zinc–bromide heavy-liquid separation; and a final Soxhlet extraction with a benzene–methanol azeotrope. Carbon, nitrogen, hydrogen, and total sulfur were run on a Thermo Flash 2000 elemental analyzer using acetanilide, sulphanilamide, and lube oil as standard checks during the analyses. Lube oil at varying weights was used as the calibration standard. Total iron was determined by inductively coupled plasma–atomic emission spectroscopy on 0.4 to 0.6 g of kerogen dissolved in a perchloric and nitric acid solution. The total iron was used to determine pyritic sulfur, which was subtracted from the total sulfur to derive organic sulfur. Analyses shown in Table 4 are the average of two to six determinations.

Stable carbon isotopes ($\delta^{13}C$) of kerogen have been shown to show no significant change with thermal maturation well into metamorphism (e.g., Landergren, 1955; Hoefs and Frey, 1976). Therefore, they are a good indicator of the original source of organic matter and depositional conditions (e.g., Maynard, 1981; Lewan, 1986) irrespective of thermal maturity. Values of $\delta^{13}C$ were determined on 0.2 to 0.6 mg of isolated kerogen that was flash combusted at 1030°C in a stream of oxygen. The generated gas was passed over copper at 600°C to remove excess oxygen and convert NO_x to N_2. Water was removed from the gas by passing it through a magnesium perchlorate trap and finally through a CarboSieve G™ column (1-m length with 5-mm outside diameter) at 90°C to separate the CO_2. The CO_2 was passively drawn by open split into a Thermo Finnigan-MAT253 isotope ratio mass spectrometer for $\delta^{13}C$ determination as described by Carter and Barwick (2011). Reported values are the mean of two or more replicate runs. Results in Table 4 show that the kerogens irrespective of thermal maturity have essentially the same $\delta^{13}C$ value, with an overall mean of –29.9‰ and standard deviation of 0.7‰. This narrow range indicates that the kerogens are from a similar source and from similar depositional conditions.

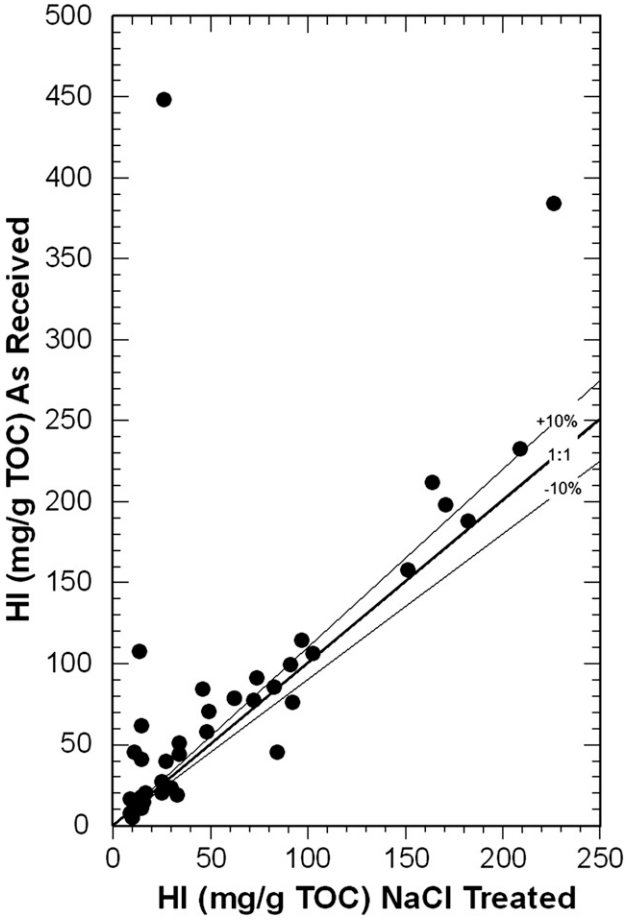

Figure 2. Plot of hydrogen index (HI) before and after cuttings underwent treatment with 20 wt. % NaCl solution to remove plastic spherical lubricant beads, wood debris, and other low-density contaminants. Solid line denotes unity agreement, and dashed lines represent plus and minus 10% deviations from unity. TOC = total organic carbon.

Klentzman Data Set

Klentzman (2009) provided HI values on Barnett Shale cuttings from 43 Encana wells. Humble Geochemical Services made these determinations using a LECO carbon analyzer and Rock-Eval II (D. Jarvie, 2014, personal communication). The location of these wells is shown in Figure 1, and the values are given in Table 5. Reflectance measurements were made by Charles Landis on samples from 18 of the wells, and only the average values as shown in Table 5 were provided by Klentzman (2009). These values are reported by Klentzman (2009) as R_o measured on whole rock.

Table 3. Mean, Standard Deviation, and Counts of US Geological Survey Reflectance Measurements (Percent Vitrinte Reflectance)

	$\%R_o$				$\%R_o$				$\%R_o$		
Sample Number	Mean	Std. Dev.	Counts	Sample Number	Mean	Std. Dev.	Counts	Sample Number	Mean	Std. Dev.	Counts
001	2.43	0.25	11	034	1.65	0.16	9	077	2.62	0.30	21
002	2.10	0.14	11	035	1.65	0.16	9	078	1.05	0.16	6
003	1.86	0.09	18	036	1.84	0.12	4	079	2.00	0.18	15
004	2.07	0.17	10	037	1.34	0.16	6	080	1.11	0.17	7
005	1.60	0.14	9	038	2.12	0.13	11	081	1.79	0.13	19
006	1.41	0.13	9	039	1.79	0.10	26	082	2.15	0.10	8
007	2.21	0.19	16	040	0.96	0.10	8	083	1.55	0.10	5
008	1.87	0.15	7	041	1.15	0.18	7	084	1.40	0.09	4
009	1.47	0.12	13	042	0.84	0.12	9	085	1.51	0.11	10
010	1.69	0.22	12	043	1.16	0.11	5	086	1.38	0.17	6
011	2.95	0.23	12	044	1.05	0.13	4	087	0.85	0.09	6
012	2.01	0.16	8	045	1.00	0.20	7	088	1.43	0.16	7
013	1.61	0.11	11	046	1.60	0.23	13	089	1.93	0.14	7
014	1.65	0.15	8	047	1.59	0.11	14	090	1.43	0.14	15
015	2.19	0.09	14	048	1.32	0.14	6	091	1.68	0.17	23
016	2.59	0.21	11	049	1.70	0.14	8	092	0.91	0.11	8
017	2.49	0.34	9	050	1.58	0.10	6	093	0.97	0.15	9
018	2.33	0.14	9	061	1.30	0.14	5	094	0.51	0.05	6
019	2.42	0.30	9	062	1.62	0.16	10	095	0.45	0.07	2
020	2.10	0.21	8	063	1.64	0.11	8	096	1.22	0.16	6
021	2.03	0.17	9	064	1.41	0.10	5	097	1.46	0.13	7
022	1.99	0.10	14	065	1.48	0.12	4	098	1.85	0.16	15
023	1.63	0.18	6	066	0.69	0.03	3	099	1.38	0.18	2
024	2.05	0.19	10	067	1.97	0.31	9	100	2.11	0.20	17
025	2.03	0.13	9	068	0.88	0.10	4	101	2.39	0.20	13
026	1.99	0.16	8	069	0.92	0.19	8	102	1.13	0.20	7
027	1.91	0.15	12	070	1.12	0.18	7	103	2.38	0.22	9
028	2.01	0.17	9	071	1.35	0.14	12	104	1.51	0.14	4
029	1.63	0.20	10	072	1.06	0.07	4			Average	9
030	2.05	0.21	11	073	0.92	0.20	4			Minimum	2
031	2.16	0.18	17	074	1.00	0.22	4			Maximum	26
032	1.90	0.41	7	075	0.86	0.11	14				
033	1.98	0.12	12	076	1.27	0.07	5				

Abbreviations: R_o = vitrinite reflectance; Std. Dev. = standard deviation.

Humble Data Set

This data set is a compilation of R_o measurements and Rock-Eval HI values used in several publications (Jarvie et al., 2005, 2007; Hill et al., 2007; Pollastro et al., 2007; Romero-Sarmiento et al., 2014). As shown in Table 6, this data set consists predominantly of $\%R_o$ values used in the construction of the $\%R_o$ map by Pollastro et al. (2007) and HI values used in the construction of the HI map by Jarvie et al. (2007). Daniel Jarvie, as then president of Humble Geochemical Services, provided a spreadsheet of the Humble Geochemical Services' data used in these maps. The provided values are reported as mean R_o with no documentation of the number of measurements made, criteria assessment of vitrinite macerals, or the petrographer(s) that made the measurements. A LECO carbon analyzer and Rock-Eval II determined TOC and programmed open-system pyrolysis data, respectively.

Hill et al. (2007) do not specify whether the HI values on the two samples used in their kinetic study were obtained by Rock-Eval II or 6, but a description of the methods used to obtain the reported mean reflectance values is presented. Data from Romero-Sarmiento et al. (2014) in Table 6 are Rock-Eval 6 HI values with a well-documented procedure for measured reflectance.

Hydrogen Index and Temperature at Maximum Rate of Hydrocarbon Generation by Various Open-System Pyrolysis Instruments

The exclusive use of Rock-Eval II for HI values in the USGS data set and the uncertainty in the type of open-system instrumentation used to obtain HI values in the other data sets encouraged a comparative study of HI values by various open-system pyrolysis instruments. Aliquots of a subset of 30 samples with Rock-Eval II HI values ranging from 5 to 478 mg S_2/g TOC were determined with Rock-Eval 6, Source Rock Analyzer (SRA), and Hawk instrumentation. The same Leco TOC given in Table 1 was used to calculate the HI from each instrument, and the HI values are shown in comparison with the Rock-Eval II HI values used in this study. The plot of HI values determined by Rock-Eval 6, SRA, and Hawk instrument versus those determined by Rock-Eval II is shown in Figure 3A. Within the ±10% error, there is generally good agreement among the different instruments and Rock-Eval II. However, the HI values determined by Rock-Eval 6 are higher than those of the Rock-Eval II. The HI values from the Hawk instruments correlate best with those of the Rock-Eval II. Although spurious HI values may occur, the overall results indicate that evaluating stages of petroleum generation with HI values determined with different instruments is not a significant issue based on these data. Carvajal-Ortiz and Gentzis (2015) reached a similar conclusion in their comparative study of Rock-Eval II and 6 on samples ranging from Devonian to Paleogene age.

The temperature at which maximum S_2 yield occurs is sometimes used as a proxy for reflectance (Jarvie et al., 2001). This practice requires well-documented data sets (e.g., Lewan and Kotarba,

Table 4. Elemental Analyses (Carbon, Hydrogen, Nitrogen, Sulfur, and Iron) and Stable Carbon Isotopes of Isolated Kerogen

	Elemental Analyses (wt. %)							Atomic			$\delta^{13}C$ (versus PDB)	
Sample Number	Nitrogen	Carbon	Hydrogen	Sulfur (Total)	Iron (Total)	Sulfur (Pyrite)	Sulfur (Organic)	H/C	H/[H + C]	S_{org}/C	Mean	Std. Dev.
025	1.26	48.70	1.73	16.77	14.60	16.77	0.00	0.42	0.298	0.000	−29.85	0.13
032	1.50	54.11	2.37	19.26	15.68	18.00	1.26	0.52	0.343	0.009	−29.92	0.00
034	1.43	54.04	2.29	19.17	16.01	18.39	0.78	0.52	0.336	0.005	−29.96	0.10
038	1.37	56.95	2.08	17.63	14.67	16.84	0.79	0.44	0.303	0.005	−28.82	0.02
040	2.08	57.77	3.03	14.80	11.77	13.51	1.29	0.63	0.385	0.008	−30.13	0.05
050	1.57	55.62	2.51	18.49	14.79	16.98	1.52	0.54	0.349	0.010	−30.09	0.05
057	1.31	51.29	1.63	20.01	16.32	18.73	1.28	0.38	0.275	0.009	−29.29	0.06
069	2.24	68.44	4.51	9.73	7.31	8.39	1.33	0.78	0.440	0.007	−30.24	0.03
070	1.91	65.09	4.05	12.95	8.93	10.25	2.70	0.74	0.426	0.016	−30.35	0.09
082	1.03	58.29	1.59	17.04	13.88	15.94	1.11	0.32	0.245	0.007	−27.75	0.06
087	2.24	68.19	4.41	10.21	7.78	8.93	1.28	0.77	0.435	0.007	−30.22	0.13
090	2.12	75.85	3.88	6.62	4.59	5.27	1.35	0.61	0.379	0.007	−30.39	0.19
092	1.46	47.27	3.15	23.06	19.43	22.30	0.75	0.79	0.442	0.006	−30.14	0.02
094	2.55	67.71	5.84	8.02	3.92	4.50	3.52	1.03	0.507	0.019	−30.56	0.09
095	2.74	68.72	5.74	7.12	3.39	3.89	3.23	0.98	0.499	0.018	−30.51	0.03
097	1.45	50.49	2.72	21.22	17.29	19.86	1.36	0.76	0.391	0.010	−30.11	0.07
											−29.90	***0.07***

Bold $\delta^{13}C$ values are mean and standard deviation of all mean kerogen values.
Abbreviations: PDB = Peedee belemnite; S_{org} = organic sulfur; Std. Dev. = standard deviation.

Table 5. Sample Location Description, Rock-Eval Hydrogen Index, and Reflectance as Reported by Klentzman (2009)

Sample Number	Well API Number	Well Name	Klentzman Number	HI (mg S_2/g TOC)	Reflectance (%R_o)
JK-1	42035301100100	J & L PARTNERS	J1	11	1.65
JK-2	42121331370000	MCMURREY RANCH UNIT A	J3	118	1.05
JK-3	42121332170000	TURNER "A"	J5	20	ND
JK-4	42217303780100	DAVIS A UNIT	J7	4	ND
JK-5	42217303950100	BAKER A UNIT	J8	6	ND
JK-6	42221310680100	STANK UNIT	J9	37	ND
JK-7	42221310700000	MILLS	J10	71	1.38
JK-8	42221311050000	STEWART UNIT	J11	86	1.35
JK-9	42221313510000	SLOCUM	J13	37	ND
JK-10	42221314600100	SLOCUM	J14	45	1.48
JK-11	42251304840100	LORE LEVIN	J15	8	2.34
JK-12	42251306370000	ANGUS	J16	10	2.33
JK-13	42251307310000	WASHMON-PIPES UNIT A	J17	7	ND
JK-14	42251307330000	PIPES KENNETH	J18	9	2.33
JK-15	42251308510000	BROCKETTE UNIT A	J19	14	ND
JK-16	42251308760000	CLASSIC OAKS UNIT	J20	7	2.12
JK-17	42337335070000	NUNNELEY A29	J22	145	0.95
JK-18	42367337990000	WILLOW	J24	24	ND
JK-19	42367338250000	MCLAIN	J25	31	ND
JK-20	42367338510100	WILLOW PARK RANCH	J26	33	1.63
JK-21	42367338570000	MITCHELL WM	J27	38	ND
JK-22	42367339260100	EFIRE	J28	55	ND
JK-23	42367340100000	FELLERS R	J29	36	1.5
JK-24	42367340630000	CLEVELAND	J30	36	ND
JK-25	42367340700000	SMALLING UNIT	J31	22	ND
JK-26	42367340950000	LEONARD O P INVESTMENTS UNIT 2	J32	42	ND
JK-27	42367341310000	HIGHLAND RANCH	J33	60	1.5
JK-28	42367341610000	TEXASBANC	J35	37	ND
JK-29	42367342610000	ASH CREEK UNIT	J36	19	ND
JK-30	42367343250000	FLOYD RANCH	J37	65	1.51
JK-31	42367343600000	LEONARD O P INVESTMENTS UNIT	J38	33	ND
JK-32	42367345380100	LYNCH	J39	30	ND
JK-33	42439312750100	GOFORTH ROBERT J	J42	32	ND
JK-34	42439313620100	SEWELL UNIT	J43	16	2.05
JK-35	42439315510000	RICHARDSON VIRGINIA UNIT	J44	38	1.48
JK-36	42439316840000	CHAPEL CREEK WEST UNIT	J45	29	ND
JK-37	42439316870000	ROCKY CREEK RANCH UNIT A	J46	30	ND
JK-38	42439317030000	MAHVASH UNIT	J47	34	ND
JK-39	42439317980000	ROCKY CREEK RANCH	J48	25	ND
JK-40	42439319920100	MERCER RANCH	J49	36	ND
JK-41	42497357250000	COLE M T	J52	84	1.16
JK-42	42497362610000	FORMAN "B"	J53	144	0.98

Abbreviations: HI = hydrogen index; ND = not determined; R_o = vitrinte reflectance; S_2 = generated petroleum (mg/g rock); TOC = total organic carbon.

2014) and does not always show a good correlation between T_{max} and measured reflectance (e.g., Wüst et al., 2013). The plot of T_{max} values determined by Rock-Eval 6, SRA, and Hawk instruments versus those determined by Rock-Eval II is shown in Figure 3B. Using an error of ±10°C, there is general agreement among the various instruments between 390°C and 480°C. However, spurious results are observed because of the difficulty in determining maximum yields from broad S_2 peaks. This is the case for all of the instruments with T_{max} values less than 380°C (shaded blue area in Figure 3B). Outside this area, there are still spurious values depending on the instrument used to determine the T_{max} values. Rock-Eval II gave no determination of T_{max} on two of the samples, but T_{max} determinations were made on the same samples with Rock-Eval 6, SRA, and Hawk instruments. The measured reflectances on these two samples were 1.93% and 2.07% R_o, but the difference in their T_{max} values is greater than 100°C and are in the reverse order expected with thermal maturity based on $\%R_o$ (Figure 3B). Two other samples gave peculiar results. One of the samples had T_{max} values that agreed among the Rock-Eval II, SRA, and Hawk instruments, but its T_{max} determined by Rock-Eval 6 fell well below 380°C. Similarly, another sample gave T_{max} values determined by Rock-Eval 6, SRA, and Hawk instruments below 380°C. Although the T_{max} determined by Rock-Eval II was greater than 380°C, its value of 425°C was too low for a measured reflectance of 2.95% R_o. It is apparent in Figure 3 that when compiling data sets from various sources with unspecified instrumentation, the HI values compare more favorably than T_{max}. As a result, this study will place more emphasis on HI than T_{max}.

RESULTS

Relationships between Percent Vitrinite Reflectance and Hydrogen Index and Temperature at Maximum Rate of Hydrocarbon Generation

A universal correlation between $\%R_o$ and various geochemical parameters is not typically possible, because the kinetics governing the change in $\%R_o$ are not the same as those governing the generation of petroleum (Lewan, 1985). Nevertheless, relationships may be derived from available data that are specific to a source rock in a specific basin. Figure 4 shows two relationships between $\%R_o$ and T_{max} for the Barnett Shale in the Fort Worth Basin using the USGS data set and the one proposed by Jarvie et al. (2001). The relationship between these two parameters for humic coals determined by Lewan and Kotarba (2014) is also shown for comparison. The difference in the relationship between humic coals and the USGS Barnett data is significant as expected and emphasizes the dependence of these relationships on types of organic matter and the need for calibration (Peters, 1986) when using T_{max} as a proxy for $\%R_o$. The relationship between T_{max} and $\%R_o$ using the USGS data set is not considered significant and is not recommended for use despite its specificity to the Barnett Shale. The difference in the Barnett relationship between that of Jarvie et al. (2001) and the USGS data are substantial (Figure 4). The USGS data show considerable scatter, with 57 samples used in the regression calculation, 23 samples interpreted as spurious (i.e., extreme outliers), and 14 samples with no instrument-determined T_{max} or values less than 350 mg/g rock. As described by Espitalié (1986), determining T_{max} becomes more difficult and less certain as the S_2 peak becomes broader and less intense with increasing thermal maturity. Based on our assessment of the various instruments used to measure T_{max} (Figure 3B), it appears this significant difference is a result of lower measured $\%R_o$ values in the Humble data set and not the T_{max} values.

Relationship between Percent Vitrinite Reflectance and Hydrogen Index

Similar to T_{max}, the relationship between reflectance and HI can vary significantly with kerogen type. However, the relationship between HI and $\%R_o$ using the USGS data set for the Barnett is more systematic, with less scatter (Figure 5A) than that of the T_{max} versus $\%R_o$ relationship (Figure 4). The power function describing this relationship is improved with the addition of the Klentzman data (Figure 5B), which agrees well with the USGS data. The exponential function derived by Olson (2008) from measured $\%R_o$ and HI data on various source rocks also shows good agreement with the USGS and Klentzman data sets (Figure 5C). In addition to the

Table 6. Sample Description, Rock-Eval Hydrogen Index, and Reflectance as Reported by Hill et al. (2007) and Romero-Sarmiento et al. (2014) and Used in the Construction of Hydrogen Index and Reflectance Maps by Jarvie et al. (2007) and Pollastro et al. (2007)

Sample Number*	Well API Number	Well Name and Number	HI (mg S_2/g TOC)	Reflectance (%R_o)
JHRP-1	42035000160000	Lynch 1	72	ND
JHRP-2	42035000170000	Clanton 1	44	1.41
JHRP-3	42035000190000	Schaeffer 1	62	ND
JHRP-4	42035000330000	Anderson 1	11	1.91
JHRP-5	42035000390000	Reichert 1	12	ND
JHRP-6	42059352010000	Sybil-Dickey "F" 1	208	ND
JHRP-7	42113000070000	Trigg Est. 1	9	1.21
JHRP-8	42121007180000	King, Rose M. Est. 1	22	ND
JHRP-9	42121007590000	Carrol, Rupert 1	44	1.02
JHRP-10	42133330380000	Dyer "464" 1	173	ND
JHRP-11	42133364220000	Alice E. Heirs 1	68	0.89
JHRP-12	42139300010000	Cockerham 1	8	ND
JHRP-13	42151308830000	Hattie Howard 180 2	216	ND
JHRP-14	42215000150000	Findley, S. B. 1	12	1.41
JHRP-15	42217000020000	Osborne 1	29	1.38
JHRP-16	42217000180000	Freeman 1	14	ND
JHRP-17	42221000520000	Little, H. B. 1	73	1.06
JHRP-18	42251000010000	Haskell, Dean et al. 1	35	1.62
JHRP-19	42251000020000	Piekoff, Nick 1	22	1.42
JHRP-20	42251000250000	Gage, Roy D. 1	39	ND
JHRP-21	42251000280000	Anderson, Nora 1	17	1.32
JHRP-22	42309000010000	1 Mattlage	23	ND
JHRP-23	42337328830000	1 Grant	299	ND
JHRP-24	42337329350000	1 Truitt	261	0.57
JHRP-25	42337329380000	1 Gaskins	257	0.59
JHRP-26	424170010200	Frank Doss 1	268	ND
JHRP-27	424253000400	1 McCann	39	1.26
JHRP-28	424390000300	1 R. B. Sharpless	48	ND
JHRP-29	424390000900	Putman & Lillian 1	19	ND
JHRP-30	424390002300	Browder 1	19	1.37
JHRP-31	424390002400	Hinton, T. R. 1	7	ND
JHRP-32	424390002500	Markum, B. L. 1	58	ND
JHRP-33	424393010700	Boaz Trust 1	22	ND
JHRP-34	424393016200	Johnson, Lottie B. 1	8	1.35
JHRP-35	424393016700	Oliver 1	13	ND
JHRP-36	424970022500	Adams 1	66	1.11
JHRP-37	424970027000	Hoyle, C. B. 1	61	1.12
JHRP-38	424970042100	Deaton 1	88	ND
JHRP-39	424970042500	East Tx. Trust 1	163	ND
JHRP-40	42497004470000	Garrett 1	13	ND
JHRP-41	42497005610000	Ross, V. D. 1	20	ND
JHRP-42	42497006790000	McGaughey 1	136	ND
JHRP-43	42497010370000	Dearman, H. H. 1	42	ND
JHRP-44	42497015320000	Mauldin, M. B. 1	129	ND
JHRP-45	42497326130000	W. C. Young 2	55	ND

(*continued*)

Table 6. Continued

Sample Number*	Well API Number	Well Name and Number	HI (mg S_2/g TOC)	Reflectance (%R_o)
JHRP-46	42497330180000	Maeyers 1	20	1.31
JHRP-47	42497331490000	Gregg 2	53	1.03
JHRP-48	42497332460000	Stevenson, Doris 1	20	ND
JHRP-49	42497332730000	Finlayson 1	16	1.15
JHRP-50	42497335640000	Sealy 3	95	ND
JHRP-51	42497335860000	Sims, T. P. 2	26	1.63
JHRP-52	42049352820000	Explo Mitcham 3	308	ND
JHRP-53	42121306780000	Blakely 1	17	2.01
JHRP-54	42059310580000	Edwards "761" 1	311	ND
JHRP-55	42417372890000	Ledbetter "FB" 1	335	ND
JHRP-56	42417373670000	Walker-Buckler "136" 2	320	ND
JHRP-57	42417374290000	Newell "10" 3	185	ND
JHRP-58	Lampasas County	Two outcrops (six samples)	475	0.48
HZKT-1	42281302030000	Moline 1	346	0.44
HZKT-2	42143000060000	St. Clarir C 1	68	1.15
RRBDTL-1	42009417870000	Wolf Frank 1	335	ND
RRBDTL-2	42193302670000	Mesquite 1	195	ND
RRBDTL-3	42237377970000	Tarrant A3	185	0.94
RRBDTL-4	42121306780000	Blakely 1	16	1.40

Abbreviations: HI = hydrogen index; ND = not determined; R_o = vitrinite reflectance; S_2 = generated petroleum (mg/g rock); TOC = total organic carbon.
*The HZKT samples are from Hill et al. (2007), the RRBDTL samples are from Romero-Sarmiento et al. (2014), and the JHRP samples are from Jarvie et al. (2007) and Pollastro et al. (2007).

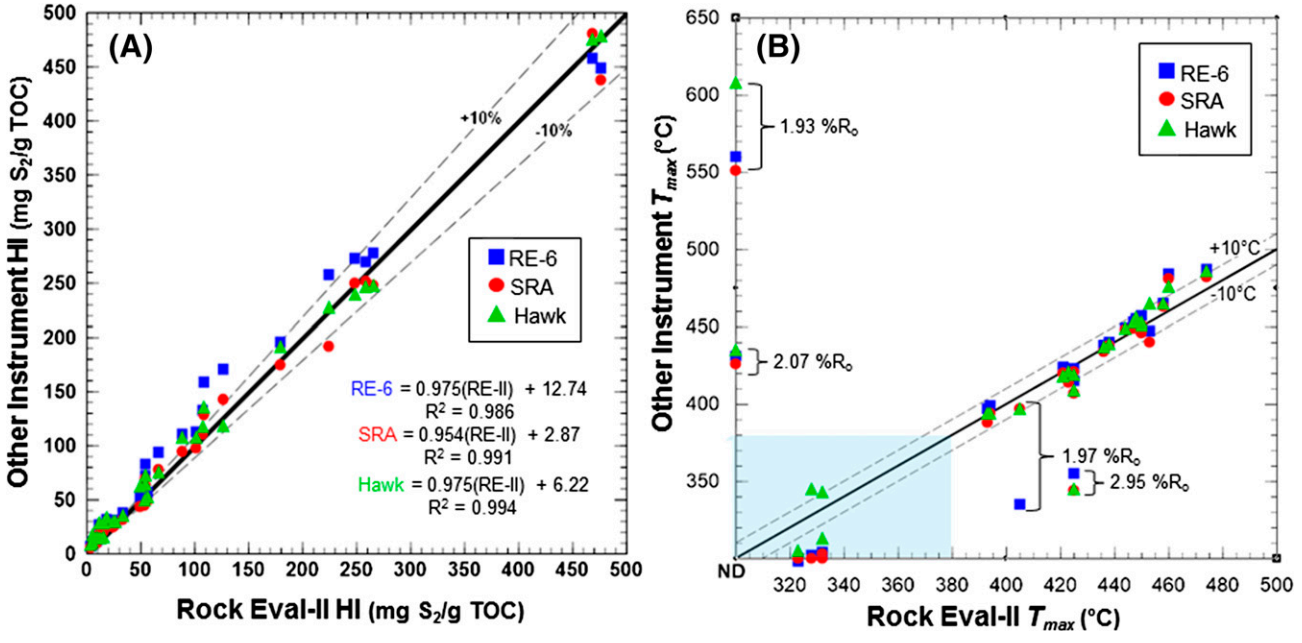

Figure 3. (A) Comparison of hydrogen index (HI) values determined by Rock-Eval II (RE-II) with Rock-Eval 6 (RE-6), Source Rock Analyzer (SRA), and Hawk instruments (Hawk). Solid line represents unity, and the dashed lines as labeled represent plus and minus 10% variations from unity based on the HI of RE-II. (B) Comparison of temperature at maximum generated petroleum rate (T_{max}) values determined by RE-II with RE-6, SRA, and Hawk. Solid line represents unity, and the dashed lines as labeled represent plus and minus 10°C variations from unity based on the T_{max} of RE-II. Shaded blue area represents area where unacceptable spurious T_{max} values occur because of broad and low-intensity generated petroleum (S_2) peaks. The T_{max} values labeled not determined from RE-II analyses have S_2 peaks less than 0.3 mg/g rock. R^2 = coefficient of determination; R_o = vitrinite reflectance; TOC = total organic carbon.

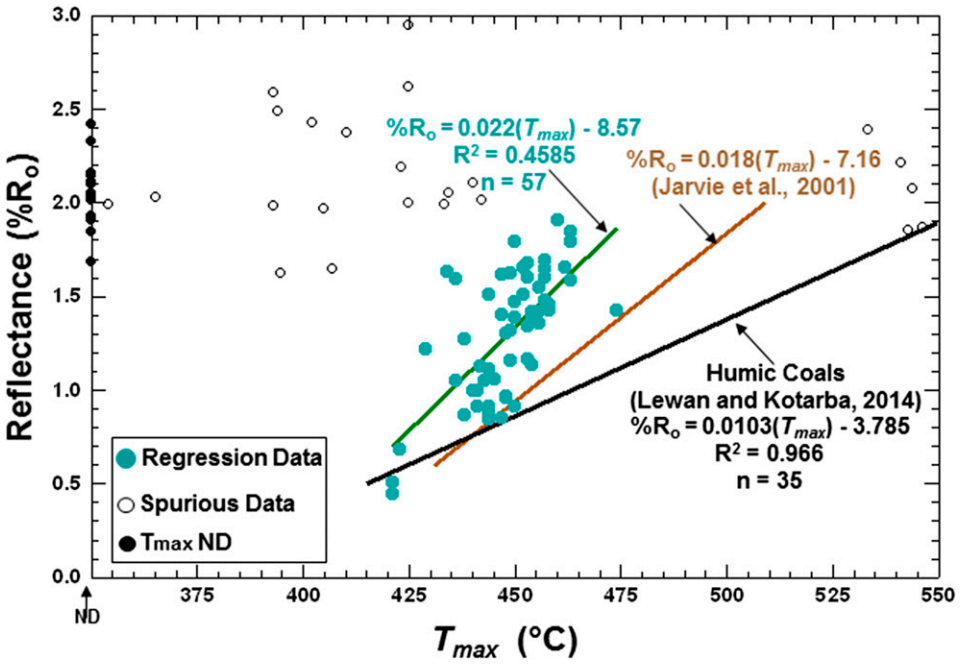

Figure 4. Plot of temperature at maximum generated petroleum rate (T_{max}) versus measured reflectance from the US Geological Survey data in this study for Barnett Shale (teal symbols used in regression, open symbols interpreted as spurious extreme outliers, and solid black symbols for generated petroleum peaks with no instrument-determined T_{max}). Relationships between T_{max} and measured reflectance by Jarvie et al. (2001) for Barnett and other non–type I bearing Paleozoic source rocks shown as dark-brown line and by Lewan and Kotarba (2014) for humic coals shown as black line. n = number of samples; ND = not determined; R_o = vitrinite reflectance; R^2 = coefficient of determination.

relationship published by Olson (2008), Figure 5C shows results from the interlaboratory study of reflectance measurements on dispersed organic matter by Hackley et al., 2015), which included analyses on 6 samples by 28 analysts in 22 laboratories from 14 countries. Excluding the low-maturity (0.31% R_o) Eocene Green River (type I kerogen; Piceance Basin) sample with its high HI (Hackley et al., 2015), results on the five samples from this interlaboratory study show good agreement with the USGS and Klentzman data sets and the relationship derived by Olson (2008).

Although the agreement of these different data sets is encouraging, the Humble data set does not agree with the relationship of the other data sets. As shown in Figure 6, reflectance values from the Humble data set are considerably lower for HI values greater than 25 mg/g TOC than for those of the USGS and Klentzman relationships. As an example, an HI value of 44 mg/g TOC equates to 1.1% R_o in the Humble expression and 1.5% R_o in the combined USGS and Klentzman expression (Figure 5B). This difference is significant in that 1.1% R_o is typically considered near the end of but within the thermal-maturity range for oil generation (0.5%–1.3% R_o; Vassorvich et al., 1974; Dow and O'Conner, 1982), and 1.5% R_o is nearing the start of oil cracking to gas at 1.5% R_o (e.g., Schenk et al., 1997). Based on our assessment of the various instruments used to measure HI (Figure 3A), it appears that this significant difference is a result of lower measured %R_o values in the Humble data set and not in the HI values. The highest %R_o value in the Humble data set is 1.9 compared with the highest %R_o value of 2.95 in the USGS data set.

These differences become more apparent in comparing the %R_o contour maps based on the USGS and Klentzman data sets (Figure 7A) with the map published by Pollastro et al. (2007) using the Humble data set (Figure 7B). Overall, the %R_o contour map by Pollastro et al. (2007) shows much lower values than the %R_o map based on the USGS and Klentzman data. As an example, the area along the Ouachita structural front in the map by Pollastro et al. (2007) (Figure 7B) has narrower %R_o contours from 1.5% to 1.7% R_o compared with the broader contours from 2.0% to greater than 2.3% R_o in the map based on the USGS and Klentzman data sets (Figure 7A). In addition, the high %R_o contour excursions in the Bosque and Tarrant Counties contoured in the map by Pollastro et al. (2007) are not observed in the contour map based on USGS and Klentzman data sets. Superimposing oil and gas production on the %R_o contoured map based on the USGS and Klentzman data sets shows that major gas production occurs at %R_o values at or greater than 1.5% R_o (Figure 8)

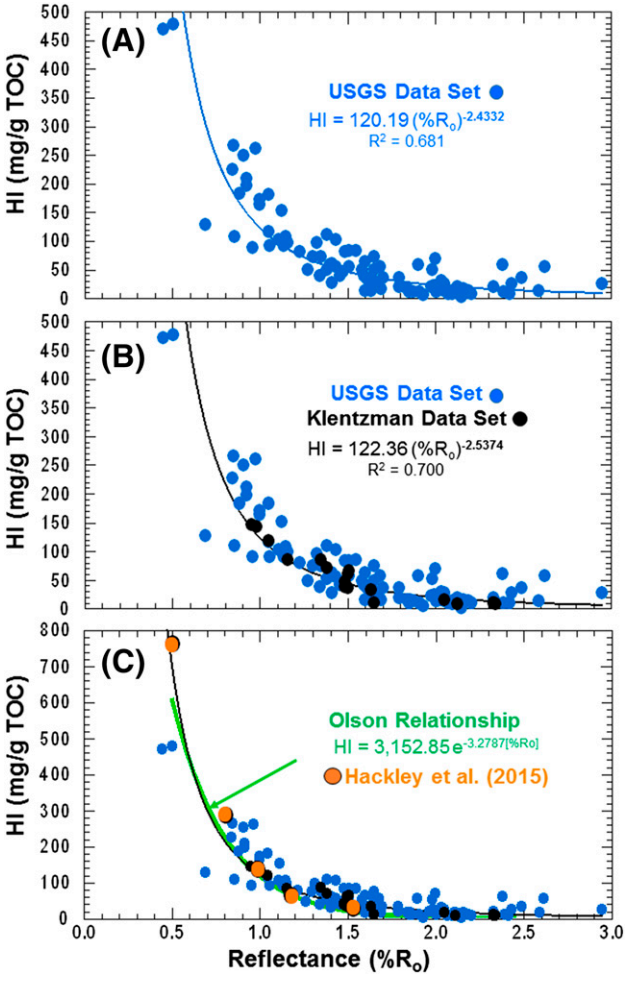

Figure 5. Plot of hydrogen index (HI) versus measured percent vitrinite reflectance (%R_o) and regression curves for (A) US Geological Survey (USGS) data set, (B) Klentzman and USGS data set, and (C) Olson (2008) relationship (green curve) with USGS and Klentzman data sets (black curve from [A]) and data from Hackley et al. (2015). R^2 = coefficient of determination; TOC = total organic carbon.

and not at 1.1% R_o as previously prescribed (Hill et al., 2007; Jarvie et al., 2007; Pollastro et al., 2007). According to rounded cumulative production for the Barnett Shale (IHS Energy, 2014), 13.5 trillion standard cubic feet (scf) of gas and 1.8 million bbl of oil have been produced in the area at or greater than the 1.5% R_o contour in Figure 8. This equates to 80% and 3% of the total cumulative produced gas and oil, respectively. Cumulative gas and oil production in the area between the 1.1% and 1.5% R_o contours contain 2.8 trillion scf and 22.7 million bbl, respectively. Cumulative gas and oil production in the area less than the 1.1% R_o contour contain only 0.5 trillion scf and 35.6 million bbl, respectively. Based on well counts (IHS Energy, 2014), the cumulative gas produced per well in the 1.5% R_o and greater area is twice that in the 1.1%–1.5% R_o area and five times that in the less than 1.1% R_o area.

Relationships between Hydrogen Index and Atomic Hydrogen/Carbon

The HI has been shown to be a good indicator of petroleum generation and a mapable parameter for the New Albany Shale in the Illinois Basin (Lewan et al., 2002) and the Bakken Formation in the Williston Basin (Lewan, 2013; Jin and Sonnenberg, 2014). Espitalié et al. (1977) has shown that the HI of a source rock is a good proxy for the atomic H/C ratio of its isolated kerogen. However, this relationship is only valid within certain ranges of thermal maturity dependent on the kerogen and source rock. Espitalié et al. (1977) observed for an assortment of source rocks at different thermal maturities that atomic H/C ratios of isolated kerogen remained constant above HI values of 450 mg/g TOC. Lewan (2013) found a similar limiting HI of 450 mg/g TOC for the upper Bakken Formation in the Williston Basin. The limiting HI value for the New Albany Shale in the Illinois Basin was 400 mg/g TOC (Lewan

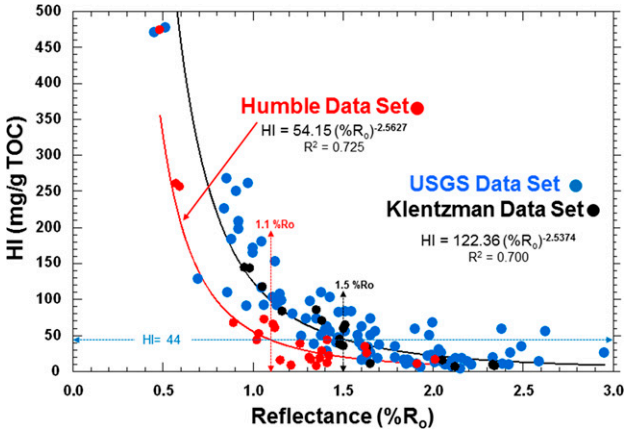

Figure 6. Plot of hydrogen index (HI) versus measured percent vitrinite reflectance (%R_o) from US Geological Survey (USGS), Klentzman, and Humble data sets. Black regression curve based on USGS and Klentzman data sets from Figure 5B, and red regression curve based on Humble data set. Construction lines refer to measured %R_o values at an HI of 42 mg/g total organic carbon (TOC) from the power expressions derived from Humble and combined USGS and Klentzman data sets. R^2 = coefficient of determination.

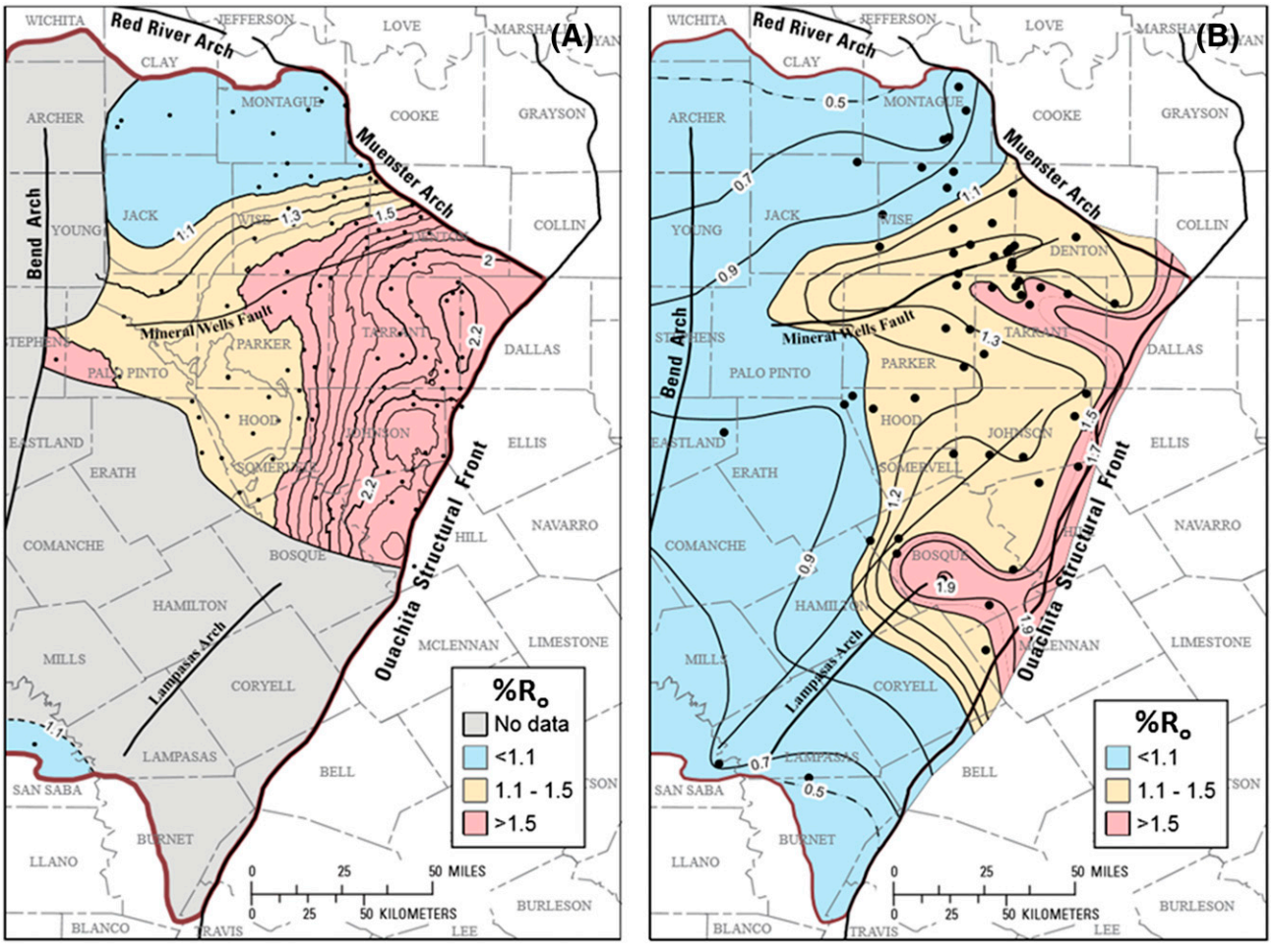

Figure 7. Percent vitrinite reflectance (%R_o) contoured maps based on (A) US Geological Survey and Klementz data sets and (B) Humble data set previously published by Pollastro et al. (2007) and used with permission of AAPG.

et al., 2002). Baskin (1997) also showed that relationships between HI values of source rocks and the atomic H/C ratios of their kerogen are only reliable up to HI values of 300 mg/g TOC in some cases. Therefore, it is critical to calibrate HI values to atomic H/C ratios of isolated kerogens at different levels of thermal maturity (e.g., Lewan et al., 2002; Lewan, 2013). Figure 9 shows this type of calibration for selected samples of Barnett Shale (Table 4) representing the full range of maturities as determined by the HI values given in Table 1. Sufficient samples at low thermal maturities were not available to accurately determine the HI value at which oil generation commences, so a value of 450 mg/g TOC was chosen in accordance with the findings of Espitalié et al. (1977) and Lewan (2013). This HI value is also used as the start of primary-gas generation, which experiments have shown to occur at essentially the same time that oil generation starts (Lewan and Henry, 1999). Baskin (1997) determines an atomic H/C ratio of 0.6, and Lewan et al. (1985) determine an atomic H/C ratio of 0.55 for the end of oil generation for both type II and IIS kerogen. Using the average of 0.575, the HI at the end of oil generation for the Barnett is 78 mg/g TOC (Figure 9). The plot of atomic H/C ratio of type II and IIS kerogen versus transformation ratio (TR) based on hydrous-pyrolysis oil yields by Lewan et al. (1985) was used to approximate an oil TR of 0.50 at an HI of 215 mg/g TOC, as shown in Figure 9. Lewan and Kotarba (2014) determined that the end of primary-gas generation from thermal decomposition of bitumen and kerogen in source rocks does not exceed an atomic H/C ratio of 0.50 irrespective of kerogen type. This places the upper limit for primary-gas generation from the Barnett at an HI of 44 mg/g TOC (Figure 9), which equates to 1.5% R_o (expression in Figure 5B).

Based on experimentally derived kinetics for low-sulfur marine oils by Tsuzuki et al. (1999) and

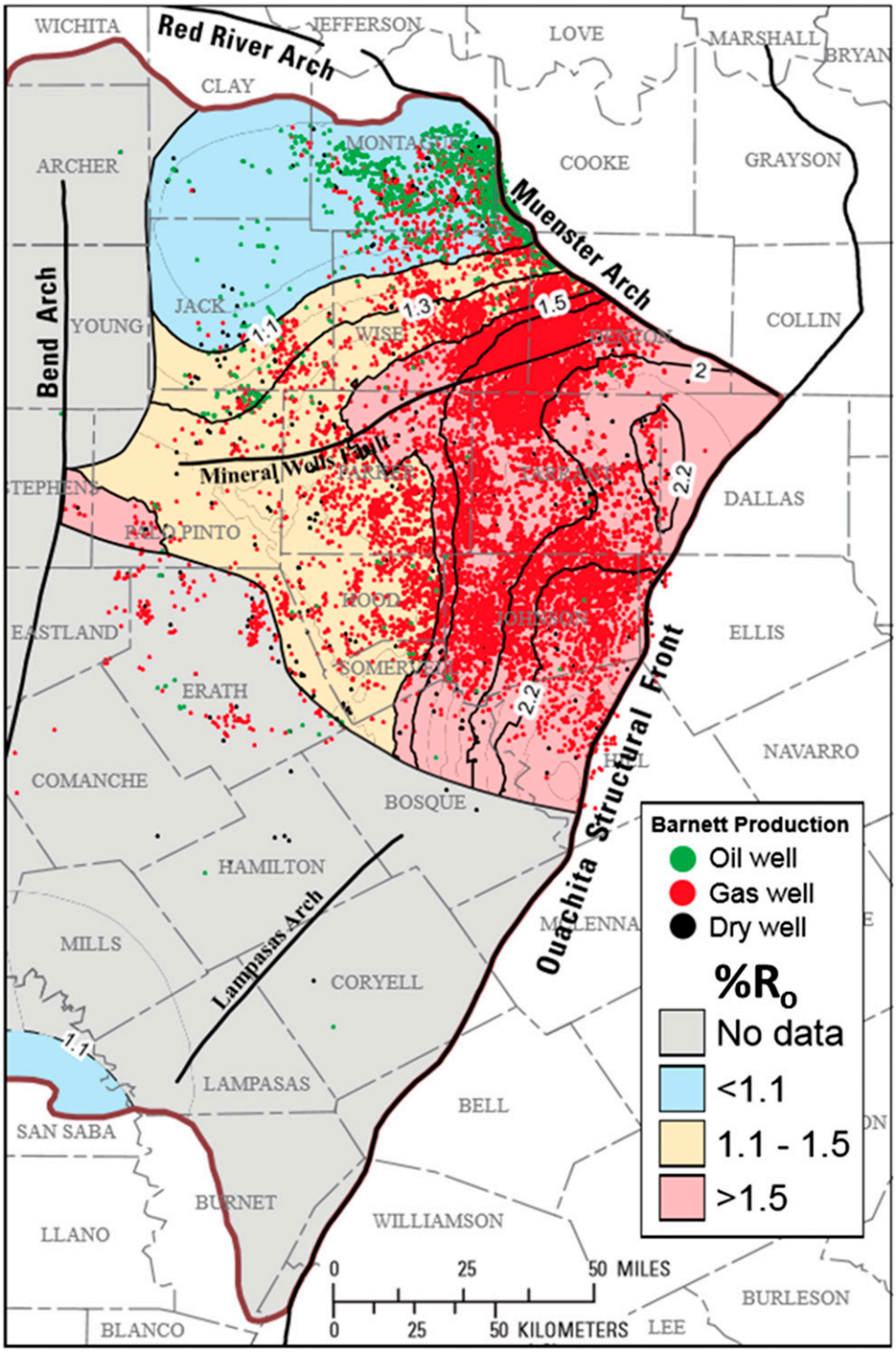

Figure 8. Percent vitrinite reflectance (%R_o) contoured map based on US Geological Survey and Klementz data sets (Figure 7A) with gas and oil wells producing from the Barnett Shale (IHS Energy, 2014). Gas wells have gas:oil ratios greater than 15,000 scf/bbl, and oil wells have gas:oil ratios less than 15,000 scf/bbl.

Schenk et al. (1997), oil cracking to gas commences at 1.5% and 1.7% R_o, respectively, for a heating rate of 2.3°C/m.y. (Figure 10). This heating rate is based on a 57 m/m.y. burial rate during the main subsidence of the Barnett Shale (326–249 Ma) in northwestern Tarrant County (Ewing, 2006) and a thermal gradient of 40°C/km (Negraru et al., 2009). Oil cracking to secondary gas under anhydrous conditions (Schenk et al., 1997), analogous to oil-wet systems, commences (TR = 0.01) at 1.5% R_o. Under hydrothermal conditions (Tsuzuki et al., 1999), analogous to water-wet systems, oil cracking to secondary gas commences (TR = 0.01) at 1.7% R_o. Hesp and Rigby (1973) and Willette (2010) have also reported greater stability of

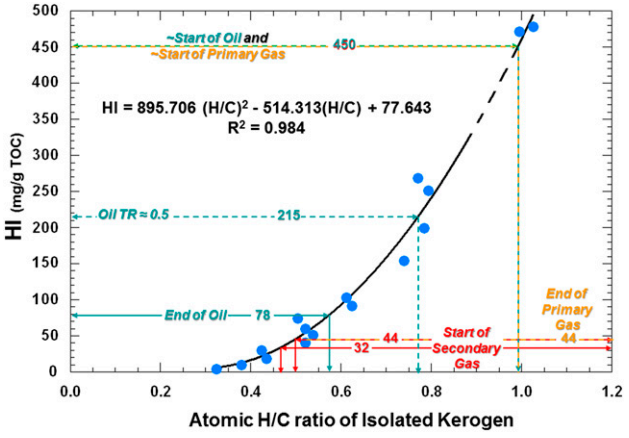

Figure 9. Plot of hydrogen index (HI) on whole rocks versus atomic H/C ratio of their isolated kerogens representing different thermal maturities (Table 4). End of oil generation based on atomic H/C ratios determined by Lewan et al. (1985) and Baskin (1997). End of primary-gas generation based on hydrous pyrolysis experiments of Lewan and Kotarba (2014). Start of secondary-gas generation from experimentally derived kinetic parameters (Schenk et al., 1997; Tsuzuki et al., 1999). R^2 = coefficient of determination; TOC = total organic carbon; TR = transformation ratio.

oil in the presence of water. These $\%R_o$ values for the start of oil cracking to secondary gas equate to HI values of 44 and 32 mg/g TOC, respectively, based on the relationship given in Figure 5B. Based on the relationship in Figure 9, this HI equates to a kerogen atomic H/C ratio of 0.50 and 0.46, respectively, for the start of secondary-gas (oil cracking) generation.

The HI values that represent the different stages of petroleum formation given in Figure 9 are contoured in Figure 11A using the HI values of all three data sets. Superimposing oil and gas production from the Barnett Shale shows general agreement with the prescribed HI contours (Figure 11B). Oil accumulations are predominant in areas above the 44-HI contour, where primary gas is generated and previously generated oil (HI < 78) remains stable. Gas accumulations are predominant below the 44-HI contour, where secondary gas is generated from the thermal cracking of previously generated oil that is no longer stable.

DISCUSSION

Vitrinite-reflectance measurements are important in calibrating thermal history and the magnitude of erosion events of sedimentary basins in which source rocks subside. However, measured $\%R_o$ by different petrographers may be the result of differences in what they identify as vitrinite (e.g., solid bitumen, reworked macerals, or vitrinite-like macerals). This is most evident in Figure 5, where four relationships of measured reflectance and HI agree with one another and a previously published one does not (i.e., Pollastro et al., 2007; i.e., Humble data set) as shown in Figure 6. Comparison of T_{max} with HI determined by different programmed open-system pyrolysis instruments (Rock-Eval II and 6, SRA, and Hawk) shows good agreement (Figure 3), which indicates that the lower measured $\%R_o$ values used by Pollastro et al. (2007; i.e., Humble data set) are problematic. This becomes an important issue, because major gas accumulations in the Barnett Shale are now occurring at 1.5% R_o instead of the previously stated 1.1% R_o (Jarvie et al., 2007). The reason for these previously reported lower $\%R_o$ values is difficult to ascertain with any certainty because of the lack of information on the petrographer and criteria used to identify measured vitrinite macerals. Speculation for

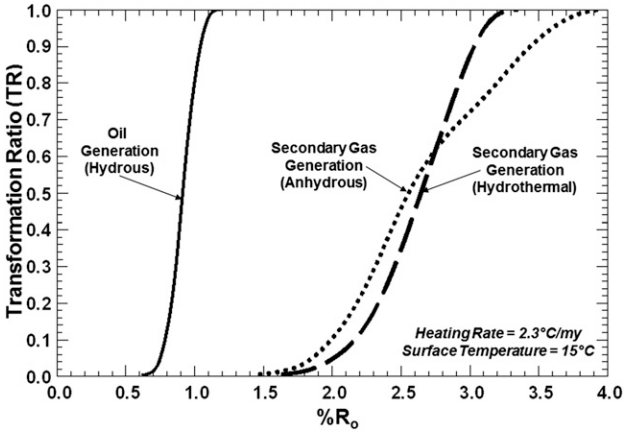

Figure 10. Burial history for a source rock and its generated oil and gas with percent vitrinite reflectance ($\%R_o$) at a heating rate of 2.3°C/m.y. and a constant surface temperature of 15°C. Calculated transformation ratios for oil generation used kinetic parameters determined from hydrous pyrolysis experiments on Woodford Shale containing type II kerogen (Lewan, 1985). Calculated transformation ratios for secondary-gas generation used kinetic parameters determined on low-sulfur marine oils for summation of C_1 through C_5 gases from hydrothermal-pyrolysis experiments (Tsuzuki et al., 1999) and for summation of C_1 through C_4 gases from anhydrous-pyrolysis experiments (Schenk et al., 1997). Presumably, both oils originated from type II kerogen. Calculated $\%R_o$ values used EASY$\%R_o$ kinetic parameters derived by Sweeney and Burnham (1990).

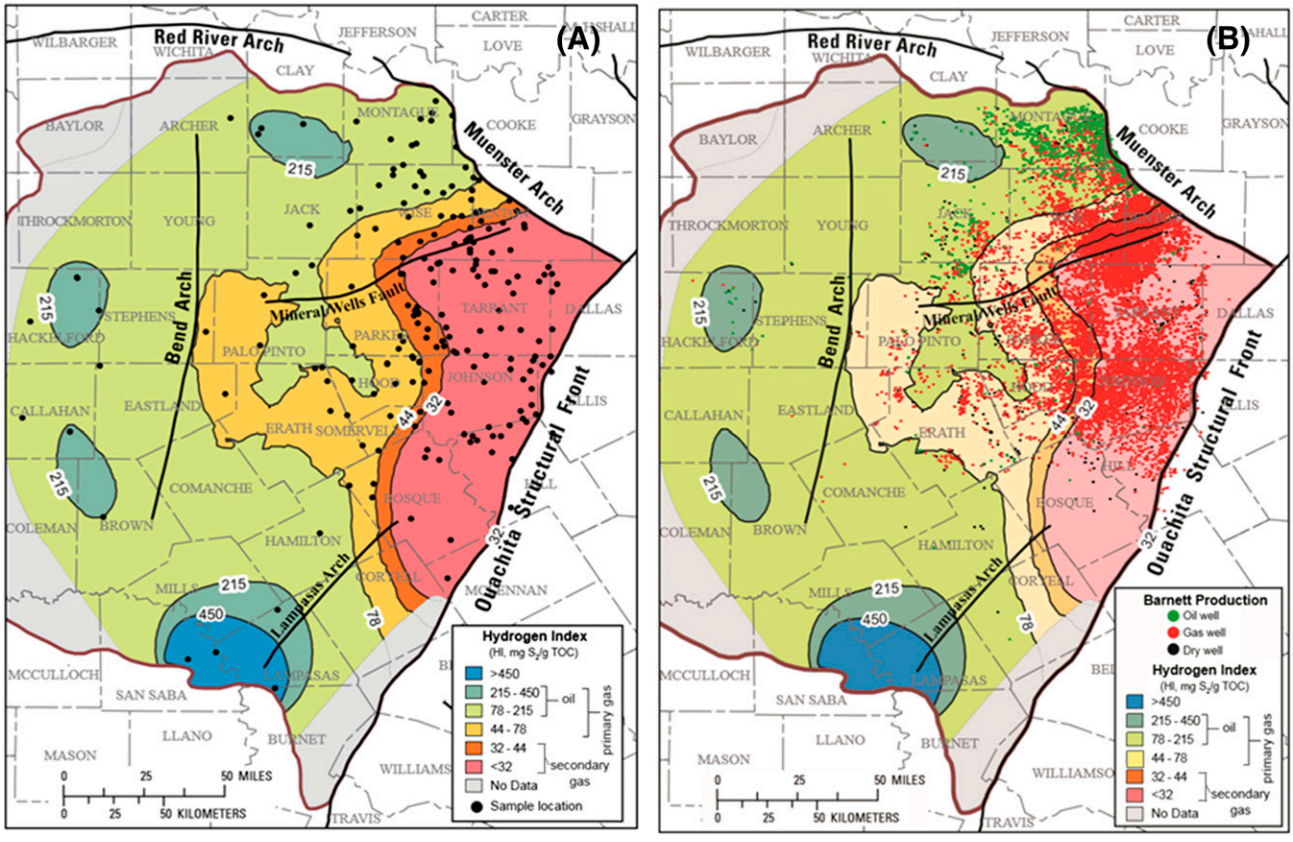

Figure 11. (A) Hydrogen index (HI) contour map of Barnett Shale based on US Geological Survey, Klentzman, and Humble data sets with contours defined by stages of petroleum formation in Figure 9. (B) The HI contour map as shown in (A) with gas and oil wells producing from the Barnett Shale (IHS Energy, 2014). S_2 = generated petroleum (mg/g rock); TOC = total organic carbon.

this difference may range from reflectance measurements on suppressed vitrinite to a petrographer's bias toward interpreting lower $\%R_o$ population modes as indigenous vitrinite.

In addition to the previously mapped low $\%R_o$ values causing issues with the use of the Barnett Shale as an analog for other gas-shale plays, the often-cited relationship between T_{max} and measured $\%R_o$ by Jarvie et al. (2001; $\%R_o = 0.018T_{max} - 7.16$) does not appear to be valid (Figure 4). The study by Wüst et al. (2013) on the Devonian Duvernay Formation of the Western Canadian Sedimentary Basin also showed a $\%R_o$ to T_{max} relationship with a high degree of scatter that was not in agreement with the relationship derived by Jarvie et al. (2001). Han et al. (2015) show that using the T_{max} relationship by Jarvie et al. (2001) results in a considerable range in the calculated $\%R_o$ from 0.7% to 1.1% R_o in a 118-m-long (387 ft) core of the Barnett Shale with no systematic change with depth; T_{max}, like HI for a source rock with type II kerogen, is an indicator of petroleum generation, which does not necessarily equate universally with a thermal stress indicator like $\%R_o$ (Lewan, 1985). Unless a well-documented calibration between measured $\%R_o$ and T_{max} is established for a given source rock within a given petroleum system, T_{max} is not a reliable proxy for measured $\%R_o$.

Vitrinite-reflectance values for the end of oil generation are influenced by kerogen type (Tissot et al., 1987) and organic sulfur content (Lewan, 1998) with proposed values as high as 1.3% R_o for the end of oil generation (Dow and O'Conner, 1982). Therefore, it is difficult to use 1.1% R_o as a threshold (Jarvie et al., 2007; Pollastro et al., 2007) for significant amounts of secondary gas generated from oil that is still being generated. This is demonstrated in Figure 10 with the comparison of oil-generation TRs with those derived from experimentally determined kinetic models specific to

oil cracking (Schenk et al., 1997; Tsuzuki et al., 1999). The TRs for oil generation are derived from hydrous-pyrolysis kinetic parameters for the Woodford Shale (Lewan et al., 1985). Type II kerogen in immature Barnett Shale has a low atomic organic-S/C ratio of 0.019 (Table 4, sample 94), which is comparable with that of the type II kerogen in immature Woodford Shale (i.e., organic-S/C ratios of 0.023; Lewan and Ruble, 2002). Regardless of whether water is present or absent during oil cracking in a maturing shale, Figure 10 shows that kinetic models predict that secondary-gas generation from oil cracking occurs at $\%R_o$ values notably greater than those for oil generation (i.e., 1.2% R_o). It is noteworthy that previously published kinetic parameters for gas generation from the Barnett Shale in gold-tube anhydrous pyrolysis either represent primary- and secondary-gas generation collectively (Hill et al., 2007) or just evaluate primary-gas generation from source-rock kerogen and bitumen (Behar and Jarvie, 2013).

The possibility that clay minerals or transition metals within a shale may result in secondary-gas generation from cracking of retained oil at relatively lower levels of thermal maturity ($\%R_o \geq 1.1$) as suggested by Hill et al. (2007) is not supported by subsequent experimental data. Willette (2010) conducted anhydrous pyrolysis experiments at 380°C for 288 hr on Smackover oil (34.0°API gravity, 1.7 wt. % S) with and without an illitic shale (61% illite, 7% chlorite, 1% kaolinite, 25% quartz, 4% feldspar, and 2% ankerite). Based on calculated surface areas of the 2-mm–sized illitic shale, the ratio of oil to mineral surface area was 0.0233 g/cm^2. The amount of gas generated with and without the illitic shale was essentially the same within the procedural error (19.2 and 19.1 wt. % of original oil, respectively). Similarly, results were reported for a quartz sand with an oil to surface-area ratio of 0.0266 g/cm^2 (Willette, 2010). With respect to transition metals in shale being catalytic in initiating early gas generation, experimental results on samples of one of the world's highest metal-bearing shales, the Permian Kupferschiefer of Poland, showed no enhanced primary- or secondary-gas generation at low thermal maturities (Lewan et al., 2008) as originally proposed by Mango (1996). Although activated Ni-oxide catalysts can crack oil at low temperatures (Mango and Elrod, 1999), Ni in an oxide phase does not occur in the reducing conditions in which source rocks are deposited or thermally matured (Lewan et al., 2008).

The best indicator of petroleum formation from bitumen generation through oil cracking to form secondary gas is the atomic H/C ratio of isolated kerogen (Lewan, 1985; Baskin, 1997; Lewan and Kotarba, 2014). However, isolating kerogen is an arduous procedure. The HI is more readily determined and may be used as a proxy for kerogen atomic H/C ratios if properly calibrated, as demonstrated for the Barnett Shale in Figure 9, New Albany Shale of the Illinois Basin (Lewan et al., 2002), and Bakken Formation of the Williston Basin (Lewan, 2013); HI as a proxy for kerogen atomic H/C ratio works well through oil and primary-gas generation, but its asymptotic trend at higher thermal maturities makes it less reliable (Figure 9). Therefore, at the higher thermal maturities where secondary-gas generation occurs, one must return to the kerogen atomic H/C ratio, which is reliable into metamorphic regimes ($\%R_o > 5.0$) and ultimately to the formation of graphite (McCartney and Ergun, 1958). As a result, HI contour maps as shown in Figure 11 provide a good representation of oil and primary-gas generation but lose their sensitivity at higher thermal maturities related to secondary-gas generation. This diminished sensitivity of HI at higher thermal maturities is most pronounced in its relationship with measured $\%R_o$ (Figure 5), where small changes in HI of 50 and 10 mg/g TOC equate to measured $\%R_o$ values of 1.4 and 2.6, respectively.

An HI map for the Barnett Shale was previously constructed by Jarvie et al. (2007; their figure 4A) using only the HI values from the Humble data set. As expected, this map has semblance to the HI map of this study (Figure 11), which includes HI data from the Humble data set along with HI values from the USGS and Klentzman data sets. Jarvie et al. (2007) do not differentiate between primary- and secondary-gas generation and suggest that secondary-gas generation starts at an HI of 87 mg/g TOC (i.e., 0.80 × 435 mg/g TOC) based on Jarvie et al. (2005). Figure 9 shows that this value remains within the stage of oil generation that ends at an HI of 78 mg/g TOC and that secondary-gas generation does not start until an HI of 44 mg/g TOC. This discrepancy in HI for the start of secondary-gas generation by Jarvie et al. (2007) is consistent with their low 1.1% R_o

value, which is also within the range for oil generation and is not indicative of secondary-gas generation.

These differences in reevaluating thermal maturity and stages of petroleum formation are particularly important in using the Barnett Shale as an analog for determining in situ shale-gas prospects in other petroleum systems. The current study advocates an HI of at least 44 mg/g TOC and a $\%R_o$ greater than 1.5 for significant in situ shale-gas accumulations sourced by secondary gas from oil cracking. With some disquiet about $\%R_o$ measurements as observed in the Humble data set, the HI limit is a more certain indicator for the start of oil cracking to secondary gas. In general, the greater the volume of source rock with thermal maturities greater than this limit (44 mg/g TOC), the greater the potential for in situ shale-gas accumulations. These higher thermal-maturity limits of 1.5% R_o and 44 mg/g TOC (i.e., HI) are more consistent with other proven gas-shale systems like the Devonian Marcellus Shale of the Appalachian Basin, Mississippian Fayetteville Shale of the Arkoma Basin, and Jurassic Haynesville Formation and Bossier Formation of the North Louisiana Salt Basin. These limits would preclude gas-shale potential in less thermally mature petroleum systems like the New Albany Shale of the Illinois Basin (Lewan et al., 2002) and Cretaceous Mowry Shale of the Powder River Basin (Anna, 2010).

CONCLUSIONS

The USGS reflectance measurements on the Mississippian Barnett Shale and their relationship with HI reported in this study are in good agreement with data by Olson (2008), Klentzman (2009), and Hackley et al. (2015). However, they do not agree with previously mapped reflectance measurements (Pollastro et al., 2007) based on the Humble data set. Reflectance measurements reported here by the USGS and those by Klentzman (2009) indicate that the Barnett Shale has reached much higher thermal maturities than previously reported, with the lower limit for secondary-gas generation in the Barnett Shale being at 1.5% R_o, rather than 1.1% R_o as previously prescribed (Jarvie et al., 2007). This difference is significant in that the higher reflectance measurements reported in this study are in agreement with secondary-gas generation from oil cracking being the main source of gases, which is in agreement with experimentally derived kinetic models. Because of these documented higher thermal maturities, mineral or transition-metal catalysis need not be invoked. More importantly, the Barnett Shale as an analog for shale gas in other basins has a thermal maturity starting at 1.5% R_o instead of the previously prescribed 1.1% R_o, which is near the end of but still within the thermal-maturity range for oil generation. This higher starting thermal maturity changes evaluations of shale-gas potential in marine petroleum systems with predominantly type II kerogen. These significant differences highlight the importance of documenting $\%R_o$ measurements and their calibration to other geochemical parameters directly related to stages of petroleum formation.

Measured $\%R_o$ showed a good and consistent relationship with HI from the USGS and Klentzman data sets, with the relationship by Olson (2008), and with data reported by Hackley et al. (2015). This relationship (i.e., $\%R_o = 4.2829[\mathrm{HI}]^{-0.276}$) is considered to give a reasonable $\%R_o$ equivalent from HI for the Barnett Shale in the Fort Worth Basin. It does not necessarily apply to other source rocks, which may have different relationships because of kerogen type or their organic-sulfur content. It is important to realize that the kinetics governing the thermal cracking of oil-prone kerogen that is responsible for diminishing HI values are not likely to be the same as those governing thermal condensation and aromatization of vitrinite and vitrinite-like macerals that are responsible for their increasing reflectance. The relationship between T_{max} and measured $\%R_o$ in the USGS data set showed considerable scatter and did not agree with the relationship prescribed by Jarvie et al. (2001; $\%R_o = 0.0180T_{max} - 7.16$).

The atomic proportionality of kerogen hydrogen to carbon (i.e., atomic H/C ratio or atomic H/[H + C] fraction) is the best parameter for evaluating stages of petroleum formation from bitumen to graphite generation. If properly calibrated, HI may serve as a good proxy for atomic proportionality of kerogen hydrogen to carbon. This proxy is good for evaluating oil and primary-gas generation, but its utility diminishes with secondary-gas generation, because the relationship becomes asymptotic at higher thermal

maturities. At these higher thermal maturities, direct measurements of atomic proportionality of kerogen hydrogen and carbon are needed to establish levels of thermal maturity for secondary-gas generation. Secondary-gas generation in the Barnett Shale started at an atomic H/C ratio of 0.50 (i.e., atomic H/[H + C] fraction = 0.333), which in the Barnett is equivalent to an HI of 44 mg/g TOC and 1.5% R_o.

REFERENCES CITED

Anna, L. O., 2010, Geologic assessment of undiscovered oil and gas in the Powder River Basin province, Wyoming and Montana, *in* L. O. Anna, ed., Total petroleum systems and geologic assessment of oil and gas resources in the Powder River Basin Province, Wyoming and Montana: US Geological Survey Series DDS-69-U, 97 p.

ASTM, 2011, ASTM D7708: Standard test method for microscopical determination of the reflectance of vitrinite dispersed in sedimentary rocks: West Conshohocken, Pennsylvania, ASTM International.

Baskin, D. K., 1997, Atomic H/C ratio of kerogen as an estimate of thermal maturity and organic matter conversion: AAPG Bulletin, v. 81, no. 9, p. 1437–1450.

Behar, F., and D. M. Jarvie, 2013, Compositional modeling of gas generation from two shale gas resource systems: Barnett Shale (United States) and Posidonia Shale (Germany), *in* J. Chatellier and D. M. Jarvie, eds., Critical assessments of shale resource plays: AAPG Memoir 103, p. 25–44.

Buchardt, B., and M. D. Lewan, 1990, Reflectance of vitrinite-like macerals as a thermal maturity index in Cambro-Ordovician Alum Shale of southern Scandinavia: AAPG Bulletin, v. 74, no. 4, p. 394–406.

Carter, J. F., and V. J. Barwick, 2011, Good practice guide for isotope ratio mass spectrometry: Bristol, United Kingdom, Forensic Isotope Ratio Mass Spectrometry Network, 48 p.

Carvajal-Ortiz, H., and T. Gentzis, 2015, Critical considerations when assessing hydrocarbon plays using Rock-Eval pyrolysis and organic petrology data: Data quality revisited: International Journal of Coal Geology, v. 152, p. 113–122, doi:10.1016/j.coal.2015.06.001.

Chaffee, A. L., R. B. Johns, M. J. Baerken, J. W. de Leeuw, P. A. Schenk, and J. J. Boon, 1984, Chemical effects in gelification processes and lithotype formation in Victorian brown coal: Organic Geochemistry, v. 6, p. 409–416, doi:10.1016/0146-6380(84)90063-9.

Dow, W. G., and D. I. O'Conner, 1982, Kerogen maturity and type by reflected light microscopy applied to petroleum exploration, *in* F. L. Staplin, W. G. Dow, C. W. D. Milner, D. I. O'Connor, S. A. J. Pocock, P. van Gijzel, D. H. Welte, and M. A. Yükler, eds., How to assess maturation and paleotemperatures: Tulsa, Oklahoma, SEPM Short Course 7, p. 133–157.

Espitalié, J., 1986, Use of Tmax as a maturation index for different types of organic matter—Comparison with vitrinite reflectance, *in* J. Burrus, ed., Thermal modelling of sedimentary basins: Paris, Technip, p. 475–496.

Espitalié, J., J. L. Laporte, M. Madec, F. Marquis, P. Leplat, J. Paulet, and A. Boutefeu, 1977, Méthode rapide de caractérisation des roches méres, de leur potential pétrolier et de leur degré d'évoluttion: Revue de l'Institut Français du Pétrole, v. 32, p. 23–42, doi:10.2516/ogst:1977002.

Ewing, T. E., 2006, Mississippi Barnett Shale, Fort Worth basin, north-central Texas: Gas-shale play with multi-trillion cubic foot potential: Discussion: AAPG Bulletin, v. 90, no. 6, p. 963–966, doi:10.1306/02090605132.

Hackley, P. C., C. V. Araujo, A. G. Borrego, A. Bouzinos, B. J. Cardott, A. C. Cook, C. Eble, et al., 2015, Standardization of reflectance measurements in dispersed organic matter: Results of an exercise to improve interlaboratory agreement: Marine and Petroleum Geology, v. 59, p. 22–34, doi:10.1016/j.marpetgeo.2014.07.015.

Han, Y., N. Mahlstedt, and B. Horsfield, 2015, The Barnett Shale: Compositional fractionation associated with intraformational petroleum migration, retention, and expulsion: AAPG Bulletin, v. 99, no. 12, p. 2173–2202, doi:10.1306/06231514113.

Hatcher, P. G., L. A. Romankiw, and J. R. Evans, 1985, Gelification of wood during coalification: 1985 International Conference on Coal Science, Sydney, Australia, October 28–31, 1985, p. 616–619.

Hesp, W., and D. Rigby, 1973, The geochemical alteration of hydrocarbons in the presence of water: Erdol Kohle-Ergas-Petrochemie Brennstoff-Chemie, v. 26, p. 70–76.

Hill, R. J., E. Zhang, B. J. Katz, and Y. Tang, 2007, Modeling gas generation from the Barnett Shale, Fort Worth Basin, Texas: AAPG Bulletin, v. 91, no. 4, p. 501–521, doi:10.1306/12060606063.

Hoefs, J., and M. Frey, 1976, The isotopic composition of carbonaceous matter in metamorphic profile from the Swiss Alps: Geochimica et Cosmochimica Acta, v. 40, p. 945–951, doi:10.1016/0016-7037(76)90143-5.

IHS Energy, 2014, June, US production and well history control databases: Englewood, Colorado, IHS Energy.

Jarvie, D. M., 2012, Shale resource systems for oil and gas: Part 1—Shale-gas resource systems, *in* J. A. Breyer, ed., Giant resources for the 21st century: AAPG Memoir 97, p. 69–87.

Jarvie, D. M., B. L. Claxton, F. Henk, and J. T. Breyer, 2001, Oil and shale gas from the Barnett Shale, Fort Worth Basin, Texas (abs.): AAPG Annual Convention, Denver, Colorado, June 3–6, 2001, accessed March 28, 2017, http://www.searchanddiscovery.com/abstracts/html/2001/annual/abstracts/0386.htm.

Jarvie, D. M., R. J. Hill, and R. M. Pollastro, 2005, Assessment of the gas potential and yields from shales: The Barnett Shale model: Oklahoma Geological Survey Circular, v. 110, p. 37–50.

Jarvie, D. M., R. J. Hill, T. E. Ruble, and R. M. Pollastro, 2007, Unconventional shale-gas system: The Mississippian Barnett Shale of north-central Texas as one model for thermogenic shale-gas assessment: AAPG

Bulletin, v. 91, no. 4, p. 475–499, doi:10.1306/12190606068.

Jin, H., and S. A. Sonnenberg, 2014, Characterization for source-rock potential of the Bakken Shale in the Williston Basin, North Dakota and Montana: AAPG Search and Discovery article 80356, accessed March 28, 2017, http://www.searchanddiscovery.com/documents/2014/80356jin/ndx_jin.pdf.

Klentzman, J. L., 2009, Geochemical controls on production in the Barnett Shale, Fort Worth Basin, M.S. thesis, Baylor University, Waco, Texas, 130 p.

Landergren, S., 1955, A note on the isotope ratio $^{12}C/^{13}C$ in metamorphosed Alum Shale: Geochimica et Cosmochimica Acta, v. 7, p. 240–241, doi:10.1016/0016-7037(55)90035-1.

Lewan, M. D., 1980, Chapter 3: Sampling techniques and the effects of weathering, *in* Geochemistry of vanadium and nickel in organic matter of sedimentary rocks, Ph.D. dissertation, University of Cincinnati, Cincinnati, Ohio, p. 47–67.

Lewan, M. D., 1985, Evaluation of petroleum generation by hydrous pyrolysis experimentation: Philosophical Transactions of the Royal Society of London A, v. 315, p. 123–134.

Lewan, M. D., 1986, Stable carbon isotopes of amorphous kerogens from Phanerozoic sedimentary rocks: Geochimica et Cosmochimica Acta, v. 50, p. 1583–1591, doi:10.1016/0016-7037(86)90121-3.

Lewan, M. D., 1997, Experiments on the role of water in petroleum formation: Geochimica et Cosmochimica Acta, v. 61, p. 3691–3723, doi:10.1016/S0016-7037(97)00176-2.

Lewan, M. D., 1998, Sulfur-radical control on petroleum formation rates: Nature, v. 391, p. 164–166, doi:10.1038/34391.

Lewan, M. D., 2013, Mapping the extent and distribution of oil formation in the upper Bakken Formation, Williston Basin (abs.): AAPG 2013 Annual Convention, Pittsburgh, Pennsylvania, May 19–22, 2013, accessed March 28, 2017, http://www.searchanddiscovery.com/abstracts/html/2013/90163ace/abstracts/lew.htm.

Lewan, M. D., and A. A. Henry, 1999, Gas-oil ratios for source rocks containing type-I, -II, -IIS, and -III kerogen as determined by hydrous pyrolysis: US Geological Survey Open-File Report 99-327, 17 p.

Lewan, M. D., M. E. Henry, D. K. Higley, and J. K. Pitman, 2002, Material balance assessment of the New Albany-Chesterian petroleum system of the Illinois basin: AAPG Bulletin, v. 86, no. 5, p. 745–777.

Lewan, M. D., and M. J. Kotarba, 2014, Thermal maturity limit for primary thermogenic-gas generation from humic coals as determined by hydrous pyrolysis: AAPG Bulletin, v. 98, no. 12, p. 2581–2610, doi:10.1306/06021413204.

Lewan, M. D., M. J. Kotarba, J. B. Curtis, D. Wiecław, and A. Piestrzyński, 2008, Evaluating transition-metal catalysis in gas generation from the Permian Kupferschiefer by hydrous pyrolysis: Geochimica et Cosmochimica Acta, v. 72, p. 4069–4093, doi:10.1016/j.gca.2008.06.003.

Lewan, M. D., and T. E. Ruble, 2002, Comparison of petroleum generation kinetics by isothermal hydrous and nonisothermal open-system pyrolysis: Organic Geochemistry, v. 33, p. 1457–1475, doi:10.1016/S0146-6380(02)00182-1.

Maier, C., and S. R. Zimmerly, 1924, The chemical dynamics of the transformation of the organic matter to bitumen in oil shale: Bulletin of the University of Utah, v. 14, p. 62–81.

Mango, F. D., 1996, Transition metal catalysis in the generation of natural gas: Organic Geochemistry, v. 24, p. 977–984, doi:10.1016/S0146-6380(96)00092-7.

Mango, F. D., and L. W. Elrod, 1999, The carbon isotopic composition of catalytic gas: A comparative analysis with natural gas: Geochimica et Cosmochimica Acta, v. 63, p. 1097–1106, doi:10.1016/S0016-7037(99)00025-3.

Maynard, J. B., 1981, Carbon isotopes as indicator of dispersal patterns in Devonian–Mississippian shales of the Appalachian Basin: Geology, v. 9, p. 262–265, doi:10.1130/0091-7613(1981)9<262:CIAIOD>2.0.CO;2.

McCartney, J. T., and S. Ergun, 1958, Optical properties of graphite and coal: Fuel, v. 37, p. 272–282.

Negraru, P. T., D. Blackwell, and M. Richards, 2009, Texas heat flow patterns: AAPG Search and Discovery article 80048, accessed March 28, 2017, http://www.searchanddiscovery.com/documents/2009/80048negraru/.

Olson, R. K., 2008, Cutting analyses, in coalbed methane and shale gas exploration strategies: Workshop for sorbed gas reservoir systems: AAPG Course 15, AAPG Annual Convention, San Antonio, Texas, April 24–25, 2008, 35 p.

Peters, K. E., 1986, Guidelines for evaluating petroleum source rocks using programmed pyrolysis: AAPG Bulletin, v. 70, no. 3, p. 318–329.

Petersen, N. F., and P. J. Hickey, 1987, California Plio-Miocene oils: Evidence of early generation, *in* R. E. Meyer, ed., Exploration for heavy oil and natural bitumen: AAPG Studies in Geology 25, p. 351–359.

Pollastro, R. M., 2007, Total petroleum system assessment of undiscovered resources in the giant Barnett Shale continuous unconventional accumulation, Fort Worth Basin, Texas: AAPG Bulletin, v. 91, no. 4, p. 551–578, doi:10.1306/06200606007.

Pollastro, R. M., D. M. Jarvie, R. J. Hill, and C. W. Adams, 2007, Geological framework of the Mississippian Barnett Shale, Barnett-Paleozoic total petroleum system, Bend arch-Fort Worth Basin, Texas: AAPG Bulletin, v. 91, no. 4, p. 405–436, doi:10.1306/10300606008.

Price, L. C., and C. E. Barker, 1985, Suppression of vitrinite reflectance by amorphous-rich kerogen—A major unrecognized problem: Journal of Petroleum Geology, v. 8, p. 59–84, doi:10.1111/j.1747-5457.1985.tb00191.x.

Rayborn, J. J., 1977, Drilling fluid lubricant: US Patent 4,063,603, December 20, 1977, 6 p.

Romero-Sarmiento, M.-F., J.-N. Rouzaud, S. Bernard, D. Deldicque, M. Thomas, and R. Littke, 2014, Evolution of Barnett Shale organic carbon structure and nanostructure with increasing maturation: Organic Geochemistry, v. 71, p. 7–16, doi:10.1016/j.orggeochem.2014.03.008.

Russell, N. J., 1984, Gelification of Victorian Tertiary soft brown coal wood: I. Relationship between chemical

composition and microscopic appearance and variation in the degree of gelification: International Journal of Coal Geology, v. 4, p. 99–118, doi:10.1016/0166-5162(84)90010-7.

Schenk, H. J., R. Di Primo, and B. Horsfield, 1997, The conversion of oil into gas in petroleum reservoirs. Part 1: Comparative kinetic investigation of gas generation from crude oils of lacustrine, marine, and fluviodeltaic origin by programmer-temperature closed-system pyrolysis: Organic Geochemistry, v. 26, p. 467–481, doi:10.1016/S0146-6380(97)00024-7.

Stout, S. A., and W. Spackman, 1987, A microscopic investigation of woody tissues in peats: Some processes active in the peatification of lingo-cellulose cell walls: International Journal of Coal Geology, v. 8, p. 55–68, doi:10.1016/0166-5162(87)90022-X.

Sweeney, J. J., and A. K. Burnham, 1990, Evaluation of a simple model of vitrinite reflectance based on chemical kinetics: AAPG Bulletin, v. 74, no. 10, p. 1559–1570.

Tissot, B., 1969, Premières données sur les mécanismes et la cinétique de la formation du pétrole dans les bassins sédimentaires. Simulation d'un schèma réactionnel sur ordinateur: Oil & Gas Science and Technology, v. 24, p. 470–501.

Tissot, B. P., R. Pelet, and Ph. Ungerer, 1987, Thermal history of sedimentary basins, maturation indices, and kinetics of oil and gas generation: AAPG Bulletin, v. 71, no. 12, p. 1445–1466.

Tsuzuki, N., N. Takeda, M. Suzuki, and K. Yokoi, 1999, The kinetic modeling of oil cracking by hydrothermal pyrolysis experiments: International Journal of Coal Geology, v. 39, p. 227–250, doi:10.1016/S0166-5162(98)00047-0.

Vassorvich, N. B., A. M. Akramkhodzhaev, and A. A. Geodekyan, 1974, Principal zone of oil formation, *in* B. Tissot and F. Bienner, eds., Advances in organic geochemistry 1973: Paris, Technip, p. 309–314.

Willette, D. C., 2010, Geologic factors responsible for the generation of natural gas and pyrobitumen (char) through the pyrolysis of crude oils, Ph.D. dissertation, Colorado School of Mines, Golden, Colorado, 548 p.

Wüst, R. A. J., P. C. Hackley, B. R. Nassichuk, N. Willment, and R. Brezovski, 2013, Vitrinite reflectance versus pyrolysis Tmax data: Assessing thermal maturity in shale plays with special reference to the Duvernay shale play of Western Canadian Sedimentary Basin, Alberta, Canada: SPE Unconventional Resources Conference and Exhibition—Asia Pacific, Brisbane, Australia, November 11–13, 2013, SPE-167031-MS, 11 p.

Xiao, X., R. W. T. Wilkins, L. Dehan, L. Zufa, and F. Jiamu, 2000, Investigation of thermal maturity of lower Paleozoic hydrocarbon source rocks by means of vitrinite-like maceral reflectance-a Tarim Basin case study: Organic Geochemistry, v. 31, p. 1041–1052, doi:10.1016/S0146-6380(00)00061-9.